

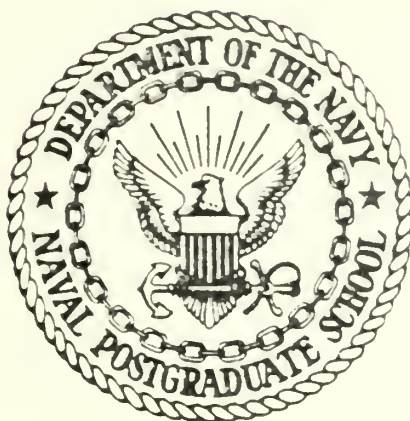
A STATISTICAL STUDY OF SYNOPTIC  
STORM ACTIVITY OVER THE  
NORTH PACIFIC IN 1975.

Gary Charles Heise



# NAVAL POSTGRADUATE SCHOOL

Monterey, California



## THESIS

A STATISTICAL STUDY OF SYNOPTIC STORM  
ACTIVITY OVER THE NORTH PACIFIC IN 1975

by

Gary Charles Heise

December 1977

Thesis Advisor:

R. L. Haney

Approved for public release; distribution unlimited.

T181449



REPORT DOCUMENTATION PAGE		READ INSTRUCTIONS BEFORE COMPLETING FORM
1. REPORT NUMBER	2. GOVT ACCESSION NO.	3. RECIPIENT'S CATALOG NUMBER
4. TITLE (and Subtitle) A Statistical Study of Synoptic Storm Activity over the North Pacific in 1975		5. TYPE OF REPORT & PERIOD COVERED Master's Thesis; December 1977
7. AUTHOR(s) Gary Charles Heise		6. PERFORMING ORG. REPORT NUMBER
9. PERFORMING ORGANIZATION NAME AND ADDRESS Naval Postgraduate School Monterey, California 93940		8. CONTRACT OR GRANT NUMBER(s)
11. CONTROLLING OFFICE NAME AND ADDRESS Naval Postgraduate School Monterey, California 93940		10. PROGRAM ELEMENT, PROJECT, TASK AREA & WORK UNIT NUMBERS
14. MONITORING AGENCY NAME & ADDRESS (if different from Controlling Office) Naval Postgraduate School Monterey, California 93940		12. REPORT DATE December 1977
		13. NUMBER OF PAGES 51
		15. SECURITY CLASS. (of this report) Unclassified
		15a. DECLASSIFICATION/DOWNGRADING SCHEDULE
16. DISTRIBUTION STATEMENT (of this Report)  Approved for public release; distribution unlimited.		
17. DISTRIBUTION STATEMENT (of the abstract entered in Block 20, if different from Report)		
18. SUPPLEMENTARY NOTES		
19. KEY WORDS (Continue on reverse side if necessary and identify by block number)		
20. ABSTRACT (Continue on reverse side if necessary and identify by block number)  A statistical analysis was made of the 00 and 12 GMT surface wind analysis prepared by Fleet Numerical Weather Central (FNWC) during 1975 to describe the synoptic storm activity over the North Pacific Ocean. Temporal variance of the surface wind components at each individual grid-point was "band passed" (approximately 2.5-6 days) using		



the filtering procedure of Blackmon (1976). Both the original winds and the time-filtered wind components were used to calculate the cube of the friction velocity and the wind stress curl. Monthly mean maps of  $u_*^3$  from the filtered wind components show clearly the location and intensity of the monthly mean synoptic storm activity during this period. Also, this measure of the synoptic storm activity was qualitatively related to the monthly mean sea surface temperature (SST) anomalies as analyzed by Namias.

A somewhat surprising result was that the monthly mean wind stress curl from the filtered wind components did not appear to have a well organized spacial pattern and did not appear to play a significant part in the generation of SST anomalies. Prior to the study, some type of relationship was thought to be probable in view of the known proportionality of wind stress curl to the Ekman pumping mechanism.





Approved for public release; distribution unlimited.

A Statistical Study of Synoptic Storm  
Activity over the North Pacific in 1975

by

Gary Charles Heise  
Captain, United States Air Force  
B.S., North Dakota State University, 1966

Submitted in partial fulfillment of the  
requirements for the degree of

MASTER OF SCIENCE IN METEOROLOGY

from the  
NAVAL POSTGRADUATE SCHOOL  
December 1977

Shells

14238

C. 1

## ABSTRACT

A statistical analysis was made of the 00 and 12 GMT surface wind analysis prepared by Fleet Numerical Weather Central (FNWC) during 1975 to describe the synoptic storm activity over the North Pacific Ocean. Temporal variance of the surface wind components at each individual grid-point was "band passed" (approximately 2.5-6 days) using the filtering procedure of Blackmon (1976). Both the original winds and the time-filtered wind components were used to calculate the cube of the friction velocity and the wind stress curl. Monthly mean maps of  $u_*^3$  from the filtered wind components show clearly the location and intensity of the monthly mean synoptic storm activity during this period. Also, this measure of the synoptic storm activity was qualitatively related to the monthly mean sea surface temperature (SST) anomalies as analyzed by Namias.

A somewhat surprising result was that the monthly mean wind stress curl from the filtered wind components did not appear to have a well organized spacial pattern and did not appear to play a significant part in the generation of SST anomalies. Prior to the study, some type of relationship was thought to be probable in view of the known proportionality of wind stress curl to the Ekman pumping mechanism.



## TABLE OF CONTENTS

I.	INTRODUCTION - - - - -	10
II.	DATA AND STATISTICAL ANALYSIS - - - - -	13
	A. DATA AND DATA PROCESSING - - - - -	13
	B. DATA FILTERING - - - - -	14
	C. CALCULATIONS - - - - -	15
III.	DISCUSSION AND RESULTS - - - - -	17
	A. DEFINITION OF STORM TRACKS - - - - -	17
	B. $CURL_Z \tau$ - - - - -	19
	C. RELATIONSHIP BETWEEN $u_*^3$ AND SST - - - - -	20
	D. RELATIONSHIP BETWEEN $CURL_Z \tau$ AND SST - - - - -	21
IV.	CONCLUSIONS - - - - -	23
	LIST OF REFERENCES - - - - -	49
	INITIAL DISTRIBUTION LIST - - - - -	50



# LIST OF FIGURES

1.	The amplitude of the 31 point band pass filter as a function of frequency. From Blackmon (1976) - - - - -	26
2.	Monthly mean friction velocity cubed ( $u_*^3$ ) from band pass filtered u and v wind components. Solid heavy lines denoted mid-latitude maximums. Contour values are .25, .5, 1., 2., 3.,.....x $10^4$ (cm/sec) <sup>3</sup> - - - - -	27
3.	Monthly mean friction velocity cubed ( $u_*^3$ ) from unfiltered u and v wind components. Solid heavy lines denote mid-latitude maximums. Contour values are .25, .5, 1., 2., 3.,.....x $10^5$ (cm/sec) <sup>3</sup> - - - - -	27
4.	Same as Fig. 2 except for February 1975. - - - - -	28
5.	Same as Fig. 3 except for February 1975 - - - - -	28
6.	Same as Fig. 2 except for March 1975 - - - - -	29
7.	Same as Fig. 3 except for March 1975 - - - - -	29
8.	Same as Fig. 2 except for April 1975 - - - - -	30
9.	Same as Fig. 3 except for April 1975 - - - - -	30
10.	Same as Fig. 2 except for May 1975 - - - - -	31
11.	Same as Fig. 3 except for May 1975 - - - - -	31
12.	Same as Fig. 2 except for June 1975 - - - - -	32
13.	Same as Fig. 3 except for June 1975 - - - - -	32
14.	Same as Fig. 2 except for July 1975 - - - - -	33
15.	Same as Fig. 3 except for July 1975 - - - - -	33
16.	Same as Fig. 2 except for August 1975 - - - - -	34
17.	Same as Fig. 3 except for August 1975 - - - - -	34
18.	Same as Fig. 2 except for September 1975 - - - - -	35
19.	Same as Fig. 3 except for September 1975 - - - - -	35





20. Same as Fig. 2 except for October 1975,  
and the paths of Typhoon Elsie and  
Flossie are shown - - - - - 36
21. Same as Fig. 3 except for October 1975 - - - - - 36
22. Same as Fig. 2 except for November 1975,  
and the paths of Typhoons June and Ida  
are shown - - - - - 37
23. Same as Fig. 3 except for November 1975 - - - - - 37
24. Same as Fig. 2 except for December 1975 - - - - - 38
25. Same as Fig. 3 except for December 1975 - - - - - 38
26. The vertical component of the January  
monthly mean wind stress curl ( $\text{curl } \tau$ )  
from band pass filtered u and v wind<sup>2</sup>  
components. Contour values are -4., -3.,  
-2., -1., 0, +1., +2., +3., +4.  $\times 10^{-9}$  dynes/cm<sup>3</sup>.  
The heavy lines are lines of zero curl, and  
gray shading denotes positive curl - - - - - 39
27. The vertical component of the January  
monthly mean wind stress curl ( $\text{curl } \tau$ )  
from unfiltered u and v wind components.  
Contour values are as in Fig. 26 except  
values are times  $10^{-8}$  dynes/cm<sup>3</sup>. The  
heavy lines are lines of zero curl - - - - - 39
28. Same as Fig. 26 except for February 1975 - - - - - 40
29. Same as Fig. 27 except for February 1975 - - - - - 40
30. Same as Fig. 26 except for March 1975 - - - - - 41
31. Same as Fig. 27 except for March 1975 - - - - - 41
32. Same as Fig. 26 except for April 1975 - - - - - 42
33. Same as Fig. 27 except for April 1975 - - - - - 42
34. January monthly mean sea surface tempera-  
ture anomalies ( $\text{SST}_{DM}$ ). Contour intervals  
are .5°C. Heavy lines are zero anomaly  
lines, warm anomaly areas are denoted by +,  
and cold anomaly areas are denoted by -.  
Dashed lines indicate monthly mean maximum  
areas of  $u_*^3$  from filtered wind as in Fig. 2 - - 43



35.	Same as Fig. 34 except for February 1975	- - - -	43
36.	Same as Fig. 34 except for March 1975	- - - - -	44
37.	Same as Fig. 34 except for April 1975	- - - - -	44
38.	Same as Fig. 34 except for May 1975	- - - - -	45
39.	Same as Fig. 34 except for June 1975	- - - - -	45
40.	Same as Fig. 34 except for July 1975	- - - - -	46
41.	Same as Fig. 34 except for August 1975	- - - - -	46
42.	Same as Fig. 34 except for September 1975	- - - -	47
43.	Same as Fig. 34 except for October 1975	- - - -	47
44.	Same as Fig. 34 except for November 1975	- - - -	48
45.	Same as Fig. 34 except for December 1975	- - - -	48



## ACKNOWLEDGEMENTS

The author would like to express his many thanks to Dr. Robert Haney for his advice and assistance in this study. Thanks also go to Mr. Steve Rinard for his assistance in data handling, and to Dr. Russell Elsberry for his advice. Data were generously supplied by FNWC and Dr. Jerome Namias of SIO. The courtesy and cooperation provided by the people working the night shift at the W. R. Church Computer Center, specifically, Mr. Edwin Donnellan, Mr. Mannus Anderson and Ms. Alice Austin have been enjoyed and appreciated.



## 1. INTRODUCTION

In studies of air-sea interaction, there have been a number of attempts to describe the relationship between anomalous synoptic-scale atmospheric circulation and patterns of anomalous sea surface temperature (SST). Synoptic scale circulation appears to be well chosen in that Simpson (1969) showed that for the middle latitudes, a significant part of air-sea exchange is due to synoptic scale disturbances. Elsberry and Camp (1977) have also shown this to be true using data from Pacific Ocean weather stations. The choice of an indicator of surface circulation has usually been in the form of sea level pressure (SLP) or upper air pressure heights from which surface winds have been derived or inferred. Namias (1972) for example, has usually employed 700 mb height data as an indicator of seasonally averaged surface circulation, while Davis (1976) has investigated the relationship between monthly mean anomalies of SLP and SST through empirical orthogonal functions. Davis (1976) concludes that the choice of SLP for a description of atmospheric circulation may be unfortunate because other atmospheric variables may show a greater influence on SST. He goes on to suggest that variables such as cloud cover, precipitation, stability, or storminess may show a greater relationship to SST than does SLP.





The primary purpose of this study has been to determine if a meaningful description of the monthly mean storminess could be derived from the total wind field. Using the 00 and 12 GMT global band surface analysis prepared by Fleet Numerical Weather Central (FNWC) during 1975, temporal variance of the surface  $u$  (zonal) and  $v$  (meridional) wind components at each individual grid point were "band passed" (approximately 2.5 - 6.0 days ) using the procedure of Blackmon (1976). This filtering process was designed to extract the circulation due to moving synoptic systems from the total circulation.

If the filtered data could be shown to adequately describe monthly mean "storminess", then the next step was to see if this measure of storminess was at least qualitatively related to SST anomalies during 1975. From both the filtered and the unfiltered wind data, the vertical component of the curl of the wind stress ( $\text{curl}_z \tau$ ) and the friction velocity cubed ( $u_*^3$ ) were computed and compared with anomalous SST fields in the North Pacific. These quantities were selected to be computed because of the well-known relationship between  $\text{curl}_z \tau$  and Ekman convergence and divergence, and the relationship between  $u_*^3$  and the mechanical mixing of the sea by the overlying atmosphere.

A secondary purpose of this study was to see if the quality and resolution of the FNWC global band wind data over the North Pacific was sufficient to warrant its use in further investigations of this type.



The remainder of this paper is devoted to describing the procedures used in data processing and statistical analysis, and to interpret the resulting patterns of  $u_*^3$  and  $\text{curl}_z \tau$  in light of the monthly mean SST anomalies. Any inferences of air-sea related activity must be qualitative because only one year's data has been considered. Also, the SST analysis is expressed as anomalies from a 20-year mean (1947-1966), generously supplied by Dr. J. Namias. There exists no long term monthly mean values of band-pass filtered  $u_*^3$  or  $\text{curl}_z \tau$  from which to determine whether any months of 1975 were normal or anomalous in these quantities. In spite of these limitations, it is hoped that this study will have provided enough clues as to whether or not this course of action is worthy of further pursuit.



## II. DATA AND STATISTICAL ANALYSIS

### A. DATA AND DATA PROCESSING

The 1975 global band surface wind analysis which is described in the U. S. Naval Weather Service Numerical Environmental Products Manual (1975) was obtained from FNWC where it had been placed in a chronological synoptic series on magnetic tape. Also, 15 date/time groups (7 1/2 days) at the end of 1974 and at the beginning of 1976 were obtained to accommodate the filtering process (to be explained later). From these data, u and v wind components were extracted from grid points on the global band from 60°N to the equator and from 100°E to 100°W (North Pacific Ocean area). The FNWC global band analysis is performed on a Mercator projection true at 22 1/2°N. The east-west grid spacing is 2.5 degrees longitude while the north-south grid spacing varies from 2.5° at the equator to 1.25 degrees at 60°N. There were 13 date/time groups missing which were interpolated linearly from preceding and succeeding map times. After these interpolations, there were 760 successive u and v wind component fields starting at 1200 GMT 24 Dec 1974 and ending at 0000 GMT 8 Jan 1976. The data were then transposed from a space representation at every synoptic time to a 380 day, twice daily time series at each of the 31x65 grid points within the North Pacific area. In order to be certain that no



errors were made in any of the data processing, representative data were verified against original synoptic maps throughout the year and were found to agree exactly.

## B. DATA FILTERING

With the data in time series at each grid point, a 31-point band pass filter described by Blackmon (1976) was applied. The equation for the filter is

$$\tilde{C}_{n,m}(t_i) = a_0 C_{n,m}(t_i) + \sum_{p=1}^{15} a_p [C_{n,m}(t_{i+p}) + C_{n,m}(t_{i-p})]$$

where  $C_{n,m}(t_i)$  represents the u or v wind component at the grid point (n,m), at the time  $t_i$ , and  $a_p$  are the coefficients for the filter.

This filter is sensitive to frequencies in the range  $0.17 \lesssim f \lesssim 0.45 \text{ days}^{-1}$  (or periods  $2.5 \lesssim T \lesssim 6.0 \text{ days}$ ), and thus is designed to extract events of the synoptic time scale. The response of the filter is shown in figure 1, and the coefficients are as follows:

$a_0$	0.2776877534
$a_1$	0.1433496840
$a_2$	-0.1020097578
$a_3$	-0.1947701551
$a_4$	-0.0923257264
$a_5$	0.0283041151
$a_6$	0.0419335015
$a_7$	0.0033466748
$a_8$	0.0041075557
$a_9$	0.0328072034
$a_{10}$	0.0304306715
$a_{11}$	-0.0020017146
$a_{12}$	-0.0191709641
$a_{13}$	-0.0096723016
$a_{14}$	-0.0001341773
$a_{15}$	-0.0030384857





### C. CALCULATIONS

Calculations of kinetic energy (KE),  $u_*^3$ , and  $\text{curl}_z \tau$  were made twice daily at every grid point using both the unfiltered and filtered wind components. Equations used for the calculations were:

$$\text{KE} = \rho_a (\tilde{u}^2 + \tilde{v}^2) / 2$$

$$u_*^3 = \left[ \frac{(\tilde{\tau}_\lambda^2 + \tilde{\tau}_\phi^2)^{1/2}}{\rho_a} \right]^{3/2}$$

$$\text{curl}_z \tau = \frac{1}{a \cos \phi} \left[ \frac{\partial \tilde{\tau}_\phi}{\partial \lambda} - \frac{\partial}{\partial \phi} (\cos \phi \tilde{\tau}_\lambda) \right]$$

where

$$\tilde{\tau}_\lambda = \rho_a C_d (\tilde{u}^2 + \tilde{v}^2)^{1/2} \tilde{u}$$

$$\tilde{\tau}_\phi = \rho_a C_d (\tilde{u}^2 + \tilde{v}^2)^{1/2} \tilde{v} .$$

Here the air density,  $\rho_a$ , was taken as a constant  $1.3 \times 10^{-3} \text{ gm cm}^{-3}$ ,  $C_d$  the non-dimensional drag coefficient as  $1.25 \times 10^{-3}$ ,  $\tilde{\tau}_\lambda$  and  $\tilde{\tau}_\phi$  are the zonal and meridional stress components, and  $\tilde{u}$  and  $\tilde{v}$  are the filtered wind components. Monthly means were computed from the twice daily computations in the standard way. Calculations using the unfiltered winds were accomplished in the same manner except  $u$  and  $v$  were used in lieu of  $\tilde{u}$  and  $\tilde{v}$ . In the finite difference approximations used to calculate  $\text{curl}_z \tau$ , centered differences on a staggered grid were used. If  $\tilde{\tau}_{\phi i, j}$  and  $\tilde{\tau}_{\lambda i, j}$  are defined on the array  $i=1, \dots, IM$  and  $j=1, \dots, JM$ , then  $\text{curl}_z \tau$  is



defined on a staggered grid by

$$\begin{aligned}
 \text{curl}_z \tau_{i,j} = & \frac{1}{a(\frac{\cos \phi_j + \cos \phi_{j+1}}{2})} \frac{1}{\Delta \lambda} [ (\frac{\tilde{\tau}_{\phi i+1,j} + \tilde{\tau}_{\phi i+1,j+1}}{2}) \\
 & - (\frac{\tilde{\tau}_{\phi i,j} + \tilde{\tau}_{\phi i,j+1}}{2}) ] - \frac{1}{\Delta \phi} [ \cos \phi_{j+1} (\frac{\tau_{\lambda i,j+1} + \tau_{\lambda i+1,j+1}}{2}) \\
 & - \cos \phi_j (\frac{\tau_{\lambda i,j} + \tau_{\lambda i+1,j}}{2}) ]
 \end{aligned}$$

where the range of  $i, j$  is  $i=1, \dots, IM-1$  and  $j=1, \dots, JM-1$ .



### III. DISCUSSION AND RESULTS

#### A. DEFINITION OF STORM TRACKS

It will be shown in this section that a representation of monthly mean storminess has been captured by calculating and plotting monthly mean values of  $u_*^3$  from the filtered wind components. This quantity was used because it is a measure of the mechanical mixing in the ocean due to the overlying atmospheric circulation, and this study has been directed at answering questions of air-sea interaction.

That the paths of monthly mean storm activity have been captured through the filtering of the  $u$  and  $v$  wind components and the subsequent mapping of monthly mean values of  $u_*^3$  can be seen, for example, by comparing figures 2, 4, and 6 with figures 3, 5, and 7. In figures 2, 4, and 6, as in all the  $u_*^3$  maps prepared from filtered wind data, there are no high values of  $u_*^3$  in the trade wind region (South of  $20^\circ\text{N}$ ) where winds are known to be quasi-steady with a minimum of disturbance activity. Figures 3, 5, and 7, on the other hand, which were calculated from the unfiltered wind data do indeed reflect the relative trade wind maximum located between  $10^\circ\text{N}$  -  $20^\circ\text{N}$ . The trade wind maximum lies south of a relative minimum area, which is in turn reflective of the mean location of the subtropical ridge. This shows that areas which are generally known to contain a minimum of storminess have small mean values



of  $u_*^3$  when calculated from the filtered wind data. On the other hand, by comparing areas of maximum monthly mean  $u_*^3$  values in the tropics with tropical cyclone paths documented by the Joint Typhoon Warning Center, Guam, it is clear that these relative maximums of  $u_*^3$  have been preserved from the original data. This can be seen in Fig. 20 and Fig. 22 where the paths of Typhoons Flossie and Elsie in October and the paths of June and Ida in November have been plotted. Maximum  $u_*^3$  areas in the tropics in Figs. 14, 16 and 18 also reflect documented tropical cyclone activity in July, August and September. Although specific extratropical cyclones were not plotted and compared in the same manner, it is reasonable to infer that if the filtering procedure has defined synoptic scale cyclone activity in these tropical cyclone cases that it has also defined extratropical cyclone activity, wherever it exists in the synoptic wind analysis.

Continuing with a comparison of  $u_*^3$  patterns in mid-latitudes calculated from filtered and unfiltered wind data, spacial differences during some months are quite pronounced. For example, in February the  $u_*^3$  maximum in the middle North Pacific from the filtered winds (Fig. 4) is located several degrees north of the  $u_*^3$  maximum based on unfiltered winds (Fig. 5). It should be noted that the hand analysis of maximum values of  $u_*^3$  come from a more detailed computer drawn plot than shown, and that the maxima analysis was done as objectively as possible. The maximum  $u_*^3$  area over northwestern North America in Fig. 5 is removed in Fig. 4,





indicating this this maximum does not result from migrating cyclone activity, but from a comparatively steady wind. Differences such as this exist in each monthly comparison. How the storm tracks are related to SST is addressed later in this paper.

#### B. $\text{CURL}_z\tau$

The objective of calculating  $\text{curl}_z\tau$  from the filtered wind data was to see if there was a contribution to Ekman pumping related solely to the mean location of cyclone propagation. Maps of the monthly mean  $\text{curl}_z\tau$ , calculated from the filtered wind data, are shown in Figs. 26, 28, 30 and 32. Typically the positive and negative areas indicate a smaller space scale and quite a different orientation which is more north-south than those resulting from the use of the unfiltered data shown in Figs. 27, 29, 31 and 33. Also there is little month-to-month spacial consistency of positive and negative areas in the case where filtered winds were used, but there is in the case where the unfiltered winds were used. Assuming the data and the filtering procedure have been satisfactory in defining the wind field due to synoptic scale storms, the rather random appearing patterns of  $\text{curl}_z\tau$  from month to month in Figs. 26, 28, 30 and 32 may indicate that the part of  $\text{curl}_z\tau$  is not important as a consistent atmospheric forcing mechanism. Another possibility, of course, is that the mean wind stress curl produced by synoptic storm activity is important, but that the 2 1/2 degree horizontal resolution



or the twice daily time resolution of the FNWC wind analysis is not fine enough to measure it. The consistency and larger scale of  $\text{curl}_z \tau$  calculations arising from the use of unfiltered wind data would indicate that the total surface circulation is important in resulting consistent synoptic scale Ekman pumping in the ocean. These patterns from the total wind data are typical of those computed and published independently in the Anomaly Dynamics Study Report (1977) for 1976.

### C. RELATIONSHIP BETWEEN $u_*^3$ AND SST

Ignoring other influences such as upwelling or advection, shortly after and at the same location where there is a maximum/minimum of wind mixing, the SST is expected to be a minimum/maximum. As was stated earlier, attempts to make correlations must be quite subjective. A goal of future studies of this type would be to see if there is a relationship between anomalies from a computed long term mean of monthly mean storm activity and anomalies of SST. The monthly mean SST anomalies provided by Namias are computed for the North Pacific from 20-60°N and are shown in Figs. 34 through 45. Also on these figures, the axis of the maximum of  $u_*^3$  from filtered wind data is shown. In spite of the limitations on this analysis mentioned above, some interesting observations can be made from these maps.

The orientation of the major axis of the warm SST anomaly which existed in the mid-Pacific for almost every month nearly parallels the isopleths of  $u_*^3$  calculated from the filtered



winds (compare Figs. 34 through 45 with the even numbered Figs. 2 through 24). This would indicate that the propensity of cyclones to track in a more zonal direction rather than meridionally in a given month may be an important factor in establishing the monthly mean SST anomalies. Some other observations may be made by comparing the  $u_*^3$  maximums and anomalous SST patterns. The  $u_*^3$  paths of storminess for the most part overlies cold SST anomalies, and, in general, have a tendency to parallel the major axis of the cold anomalies. This looks particularly good in some months such as June, July, August, November and December and not quite as good in September for example over the western Pacific. If the long-term climatological values of  $u_*^3$  were known, the hypothesis that band pass filtered  $u_*^3$  values are a major contribution to SST anomalies could be tested more fully.

#### D. RELATIONSHIP BETWEEN $\text{CURL}_Z\tau$ AND SST

The horizontal scale of positive and negative areas of  $\text{curl}_Z\tau$  from the filtered winds are not only smaller than those from the unfiltered winds, but also smaller than the scale of the SST anomalies, at least in 1975. This is perhaps more evidence that, as discussed earlier,  $\text{curl}_Z\tau$  from migrating systems alone is perhaps unimportant to large-scale Ekman pumping. Although four figures of monthly mean values of  $\text{curl}_Z\tau$  from the total wind field have been included in this paper, it has not been the purpose of this study to relate  $\text{curl}_Z\tau$  from the total wind field to SST. This is being investigated by the Anomaly Dynamics Study (ADS) group who have



recently published results on this subject in the ADS Report (1977). Suffice it to say at this point, monthly mean values of wind stress curl from the total wind and SST anomalies are of the same general size so a relationship may be indicated in view of this evidence.





#### IV. CONCLUSIONS

By temporal filtering of the 1975 FNWC global band surface wind analysis and through subsequent computations for monthly mean values of  $u_*^3$  and  $\text{curl}_z \tau$ , two reasonably conclusive results have been shown.

First, the band pass filtered  $u_*^3$  patterns have been shown to be a measure of mid-latitude synoptic disturbance activity. In relating this storminess or lack of it to anomalously cold or warm SST patterns, there appears to be a relationship between the major axis of the SST anomaly patterns and the isopleths of band pass filtered  $u_*^3$ . This suggests that both the location and the intensity of synoptic storm activity during a month are important factors in determining SST anomalies.

The second reasonably conclusive result is that the monthly mean wind stress curl, due to storm activity alone, shows little or no relationship to SST anomalies. If Ekman pumping contributes to anomalous values of SST, then the contribution must be related to the stress produced by the monthly mean total surface circulation.

The results of this study are consistent with a picture of the atmosphere forcing the ocean and not the other way around. Maximum monthly mean storminess (band pass filtered  $u_*^3$ ) tended to overlies the cold SST anomalies. If the ocean



were forcing the atmosphere, one might expect that the maximum storminess, in mid-latitudes, would lie in the region of maximum baroclinity in the SST field which would be between the warm and cold SST. These new results are therefore similar to the SST/SLP correlation study conducted by Davis (1976) in which it was generally concluded that winds associated with monthly mean SLP anomalies in the atmosphere forced monthly mean SST anomalies in the ocean. What was not concluded by Davis was whether this forcing resulted from only vertical mixing and anomalous heat fluxes, or whether it resulted from advection or Ekman pumping, or some combination of processes. The approach used in this study for defining monthly mean storminess through monthly mean values of band pass filtered  $u_*^3$  indicates that this quantity may be a good indicator of anomalous values of SST, and thus this approach may merit further study. If a long-term mean of band pass filtered  $u_*^3$  were developed, then monthly anomalies of this quantity could be compared directly with anomalies of SST. Since  $u_*^3$  is a measure of the mechanical stirring of the upper ocean by the atmosphere, one could then perhaps better deduce the proportion of the monthly mean SST anomaly that is due solely to storm-induced vertical mixing.

Another conclusion of this study is that FNWC global band surface winds are an adequate source to define mid-latitude storminess over the North Pacific Ocean. Some effort has already begun at FNWC to compile some 20 years of surface wind data on the synoptic time scale. Monthly means of band pass filtered  $u_*^3$  could be established from this data source.



It would appear to be a logical conclusion to proceed with this work for the purpose of further study in the relationship of atmospheric forcing to varying values of SST. As a caution, one shortcoming of this type of approach is the basic assumption that the anomalous atmospheric forcing is the only important factor. Surely the oceanic thermal structure (or anomalous structure) and even the seasonal evolution of the oceanic thermal structure determine the oceanic response as well. Elsberry and Camp (1977) have shown that the same atmospheric forcing produces a much larger SST response in September than it does in December, and this is no doubt true in other months as well. The ADS group is now involved in resolving this thermal structure through the processing of increased data coverage in the middle Pacific. Through this new data, perhaps the effects of atmospheric forcing and oceanic thermal structure can be combined to further resolve the interrelationships of these variables and SST.



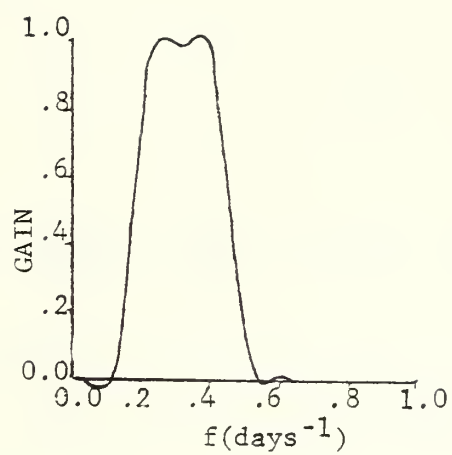


Figure 1. The amplitude of the 31 point band pass filter as a function of frequency. From Blackmon (1976).





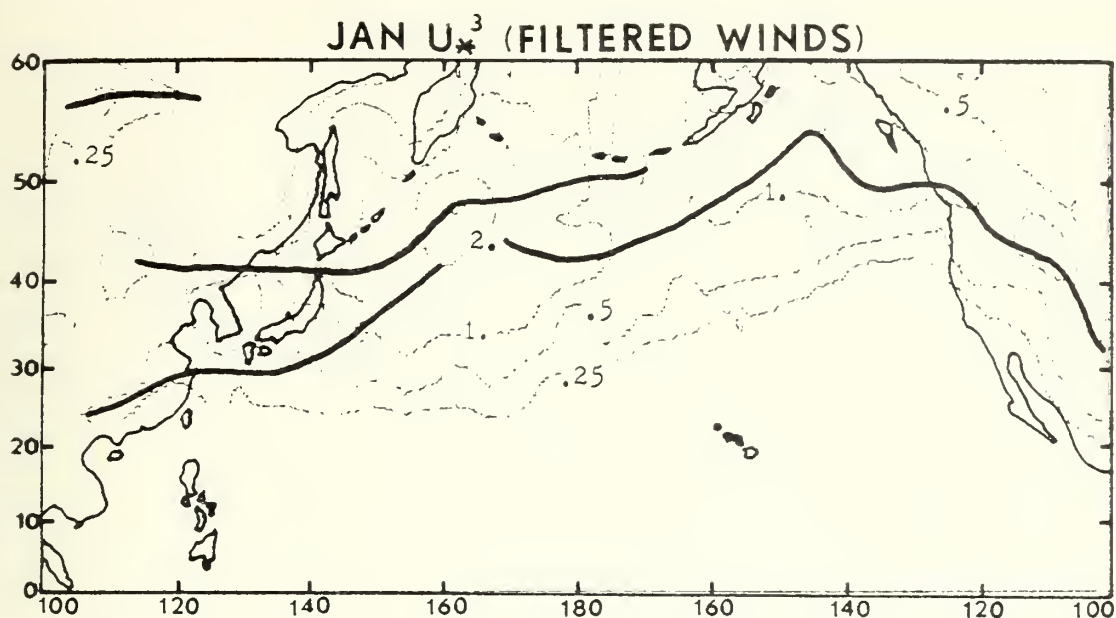


Figure 2. Monthly mean friction velocity cubed ( $u_*^3$ ) from band pass filtered u and v wind components. Solid heavy lines denoted mid-latitude maximums. Contour values are .25, .5, 1., 2., 3., ....  $\times 10^4$  (cm/sec)<sup>3</sup>.

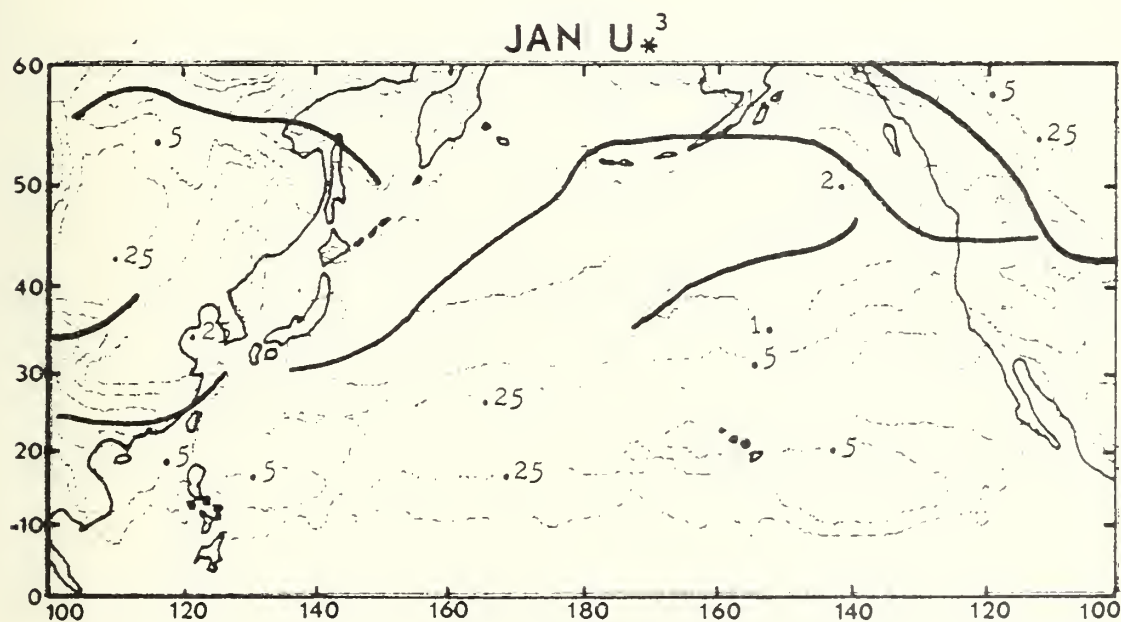


Figure 3. Monthly mean friction velocity cubed ( $u_*^3$ ) from unfiltered u and v wind components. Solid heavy lines denote mid-latitude maximums. Contour values are .25, .5, 1., 2., 3., ...  $\times 10^5$  (cm/sec)<sup>3</sup>.



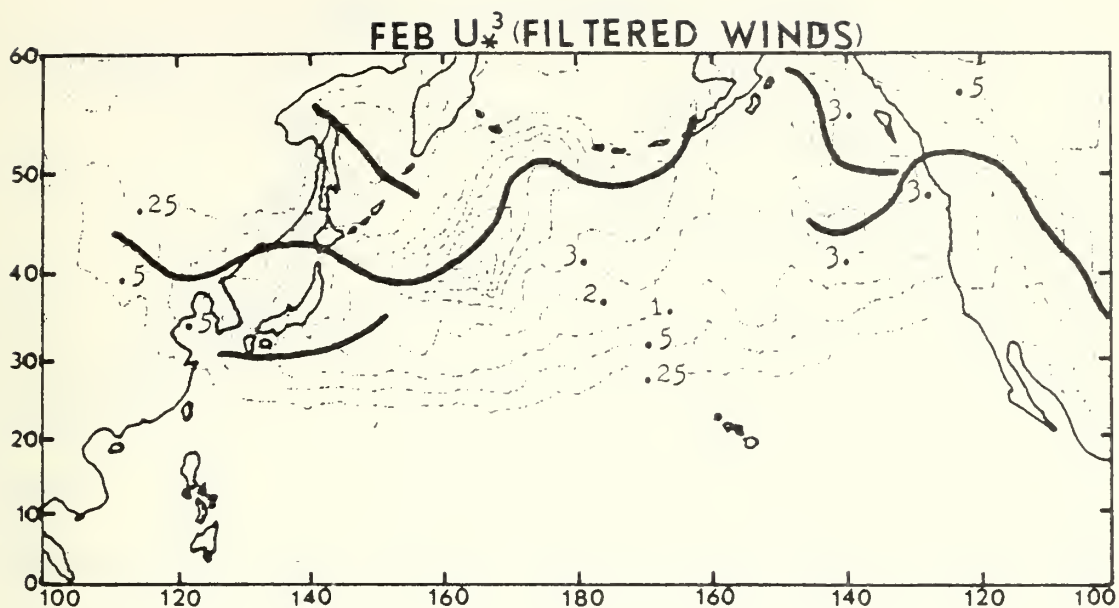


Figure 4. Same as Fig. 2 except for February 1975.

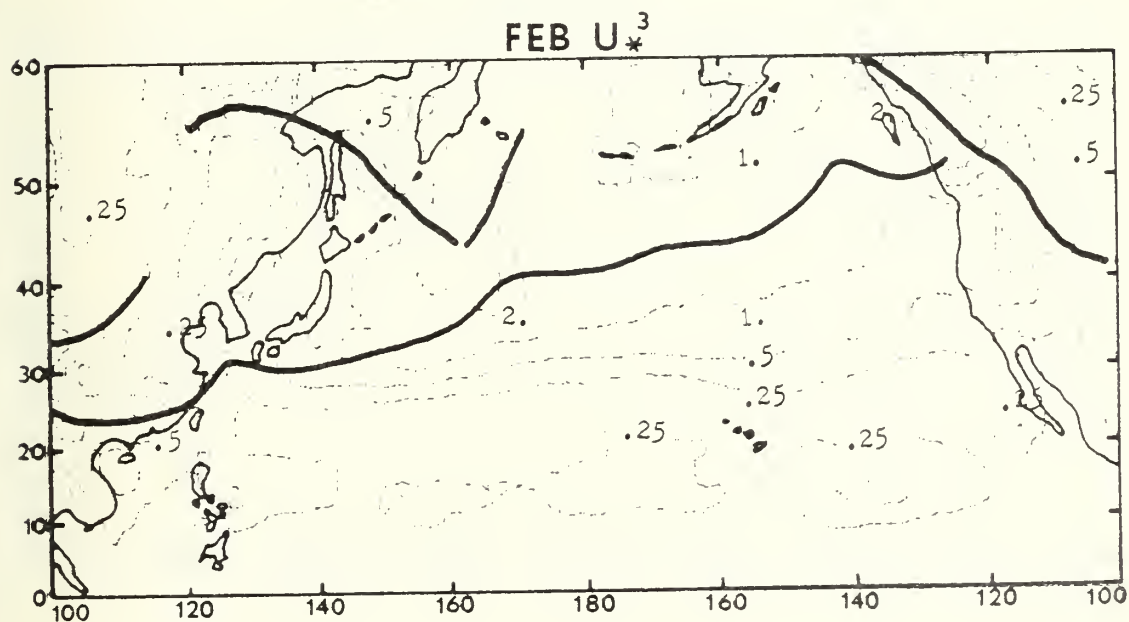


Figure 5. Same as Fig. 3 except for February 1975.



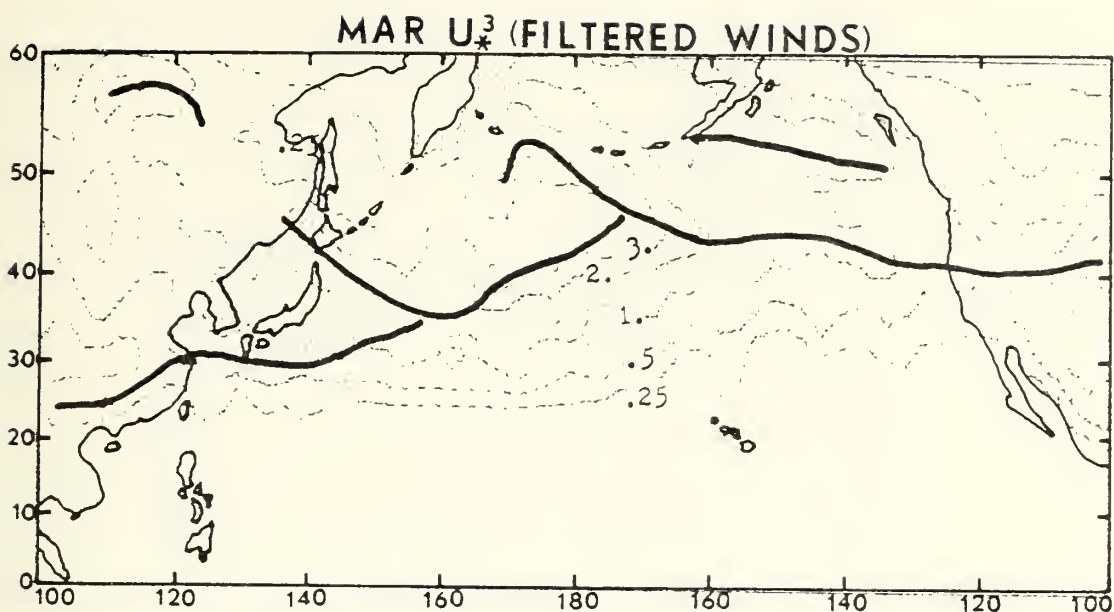


Figure 6. Same as Fig. 2 except for March 1975.

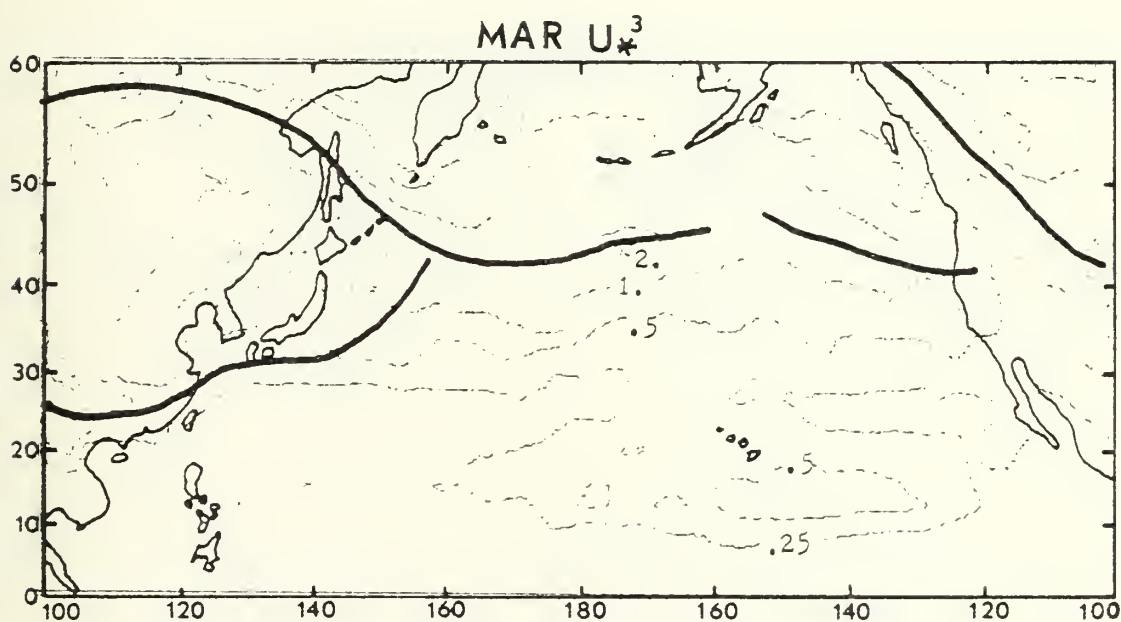


Figure 7. Same as Fig. 3 except for March 1975.



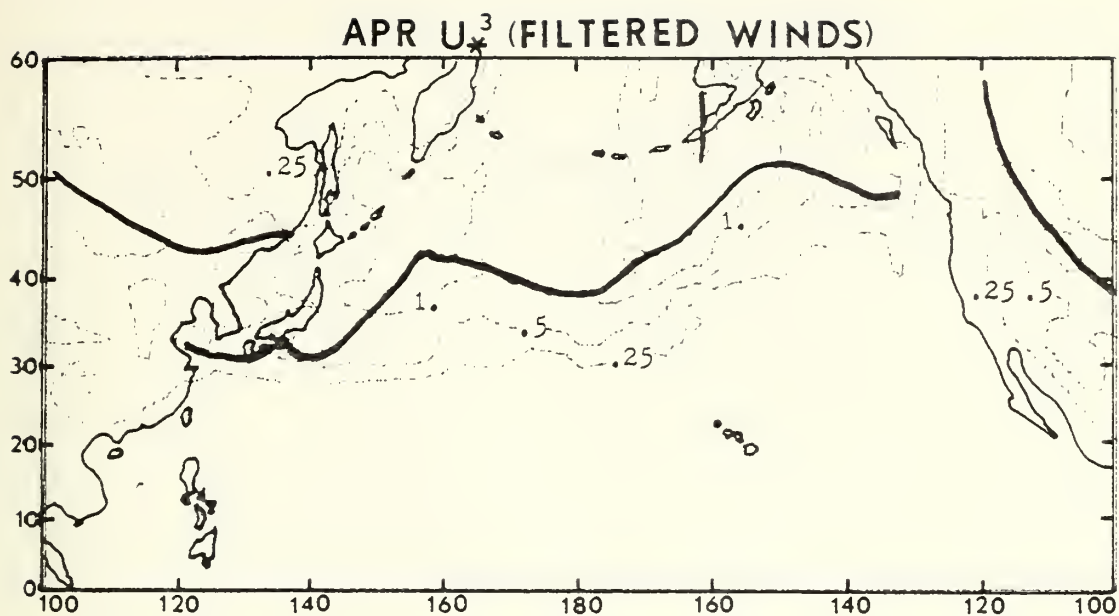


Figure 8. Same as Fig. 2 except for April 1975.

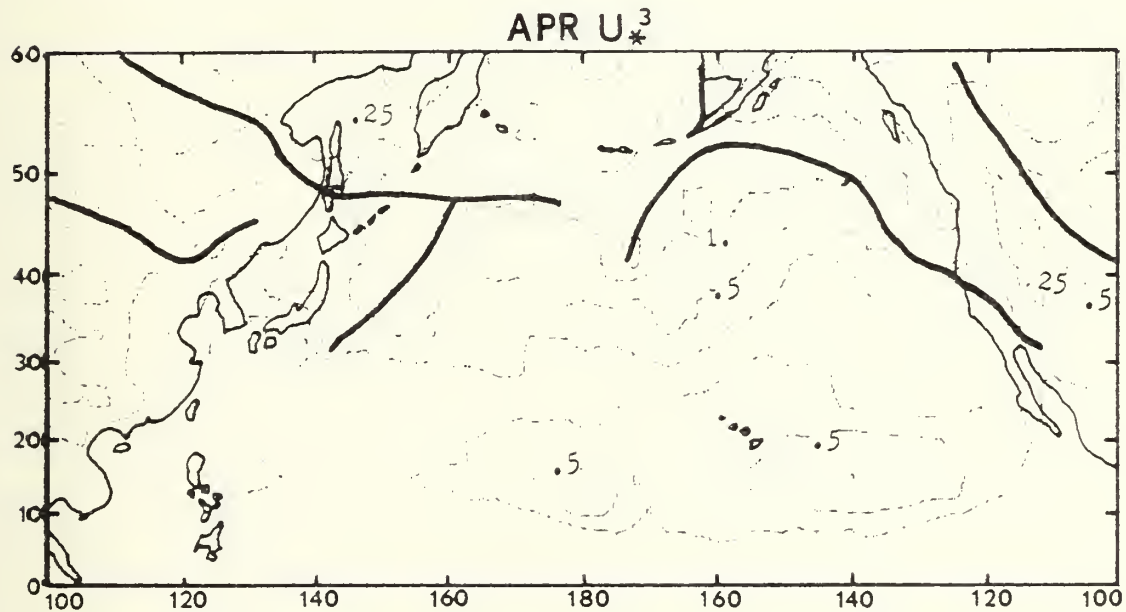


Figure 9. Same as Fig. 3 except for April 1975.





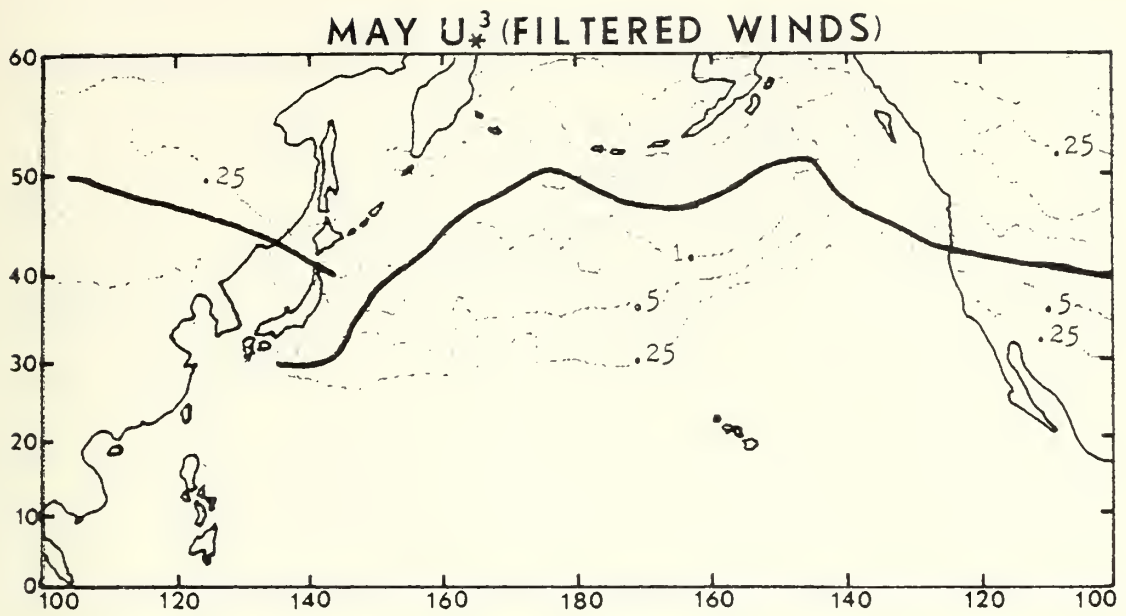


Figure 10. Same as Fig. 2 except for May 1975.

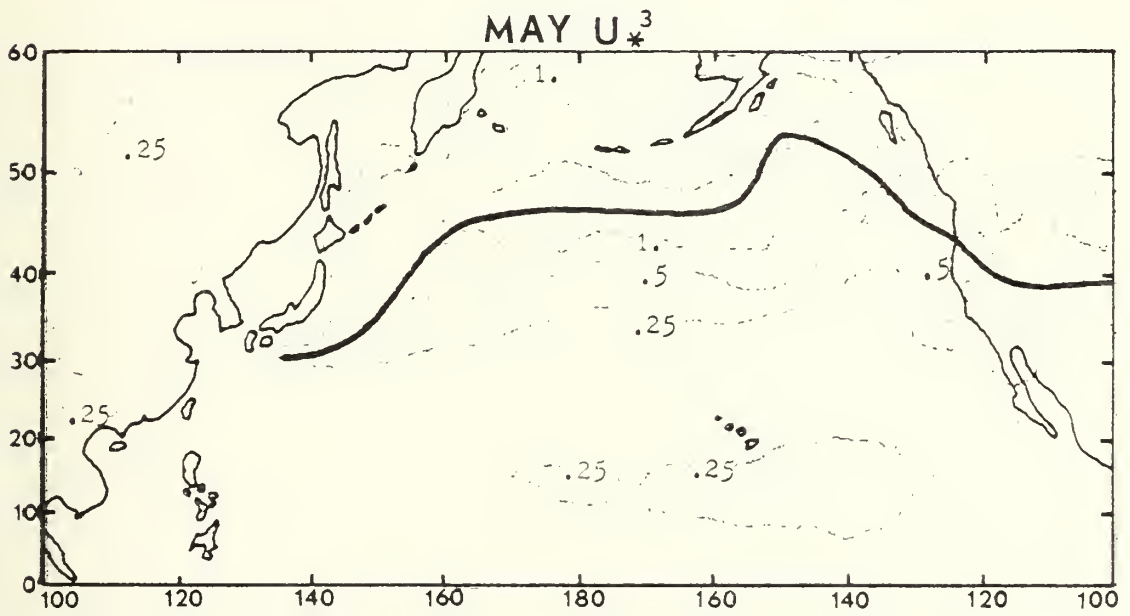


Figure 11. Same as Fig. 3 except for May 1975.



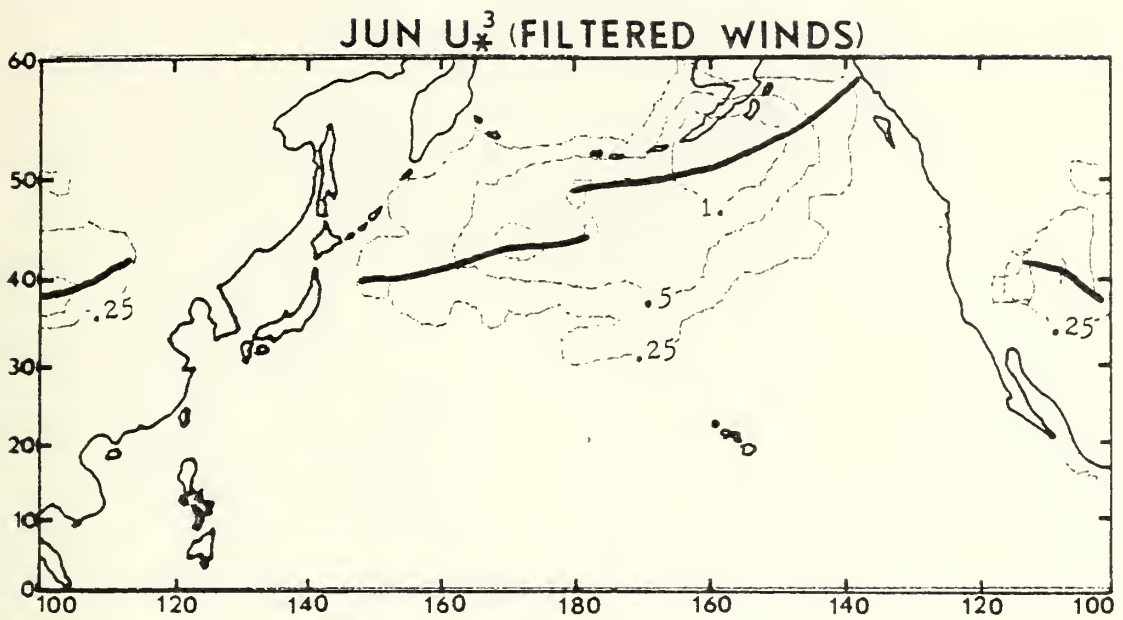


Figure 12. Same as Fig. 2 except for June 1975.

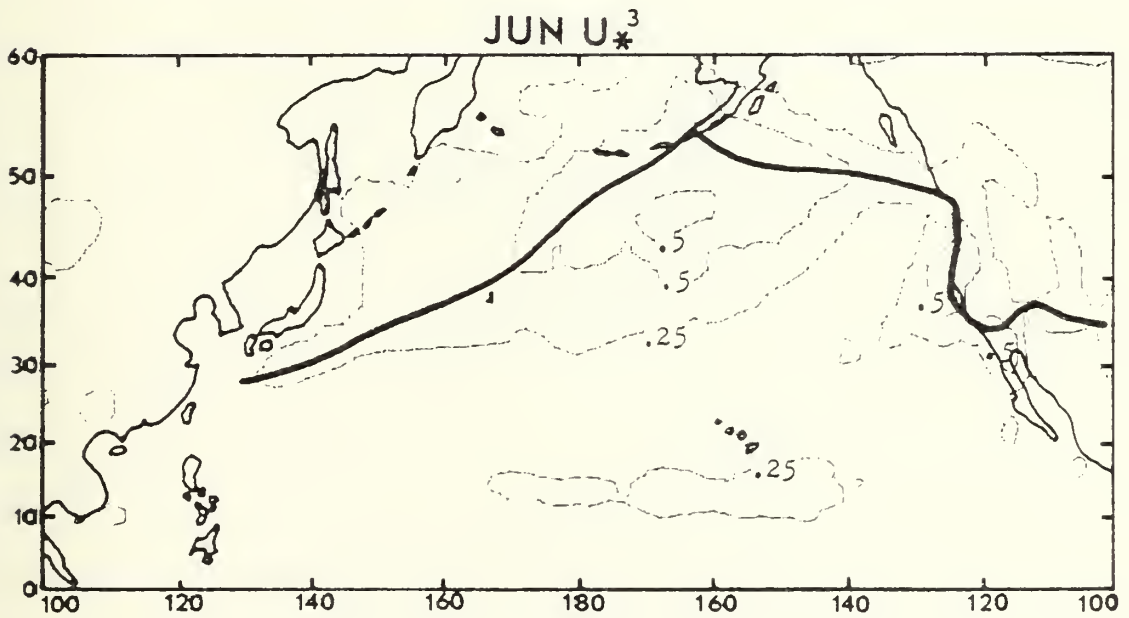


Figure 13. Same as Fig. 3 except for June 1975.



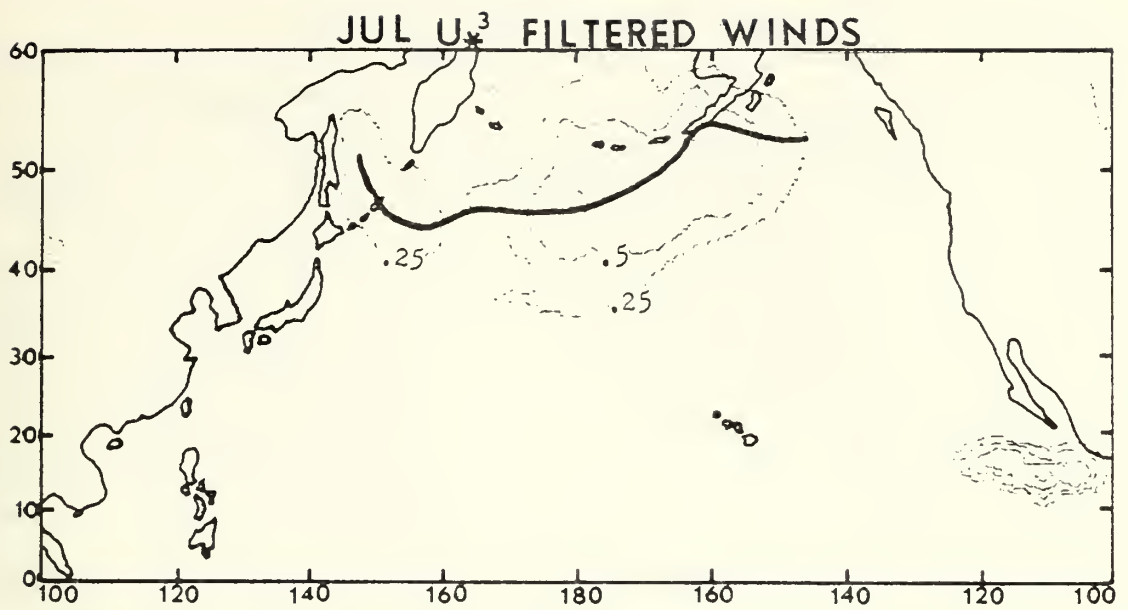


Figure 14. Same as Fig. 2 except for July 1975.

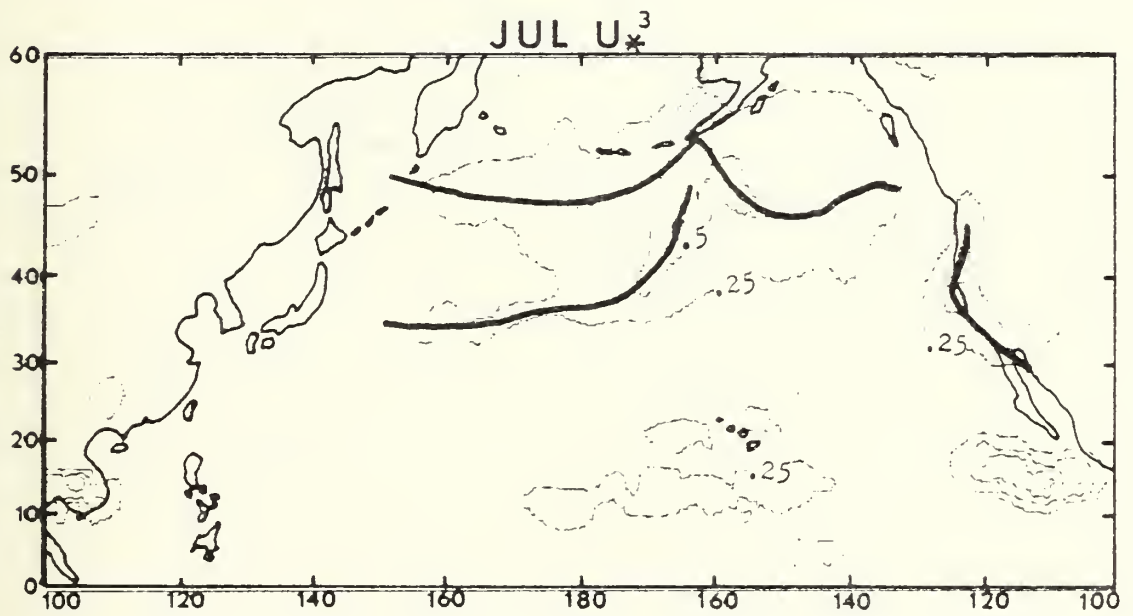


Figure 15. Same as Fig. 3 except for July 1975.



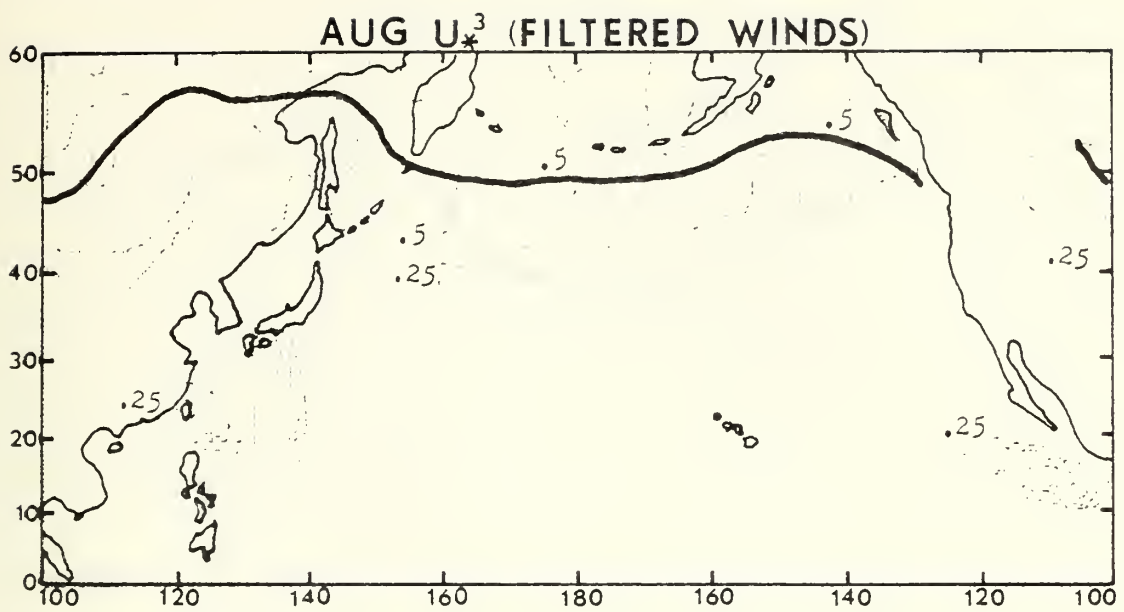


Figure 16. Same as Fig. 2 except for August 1975.

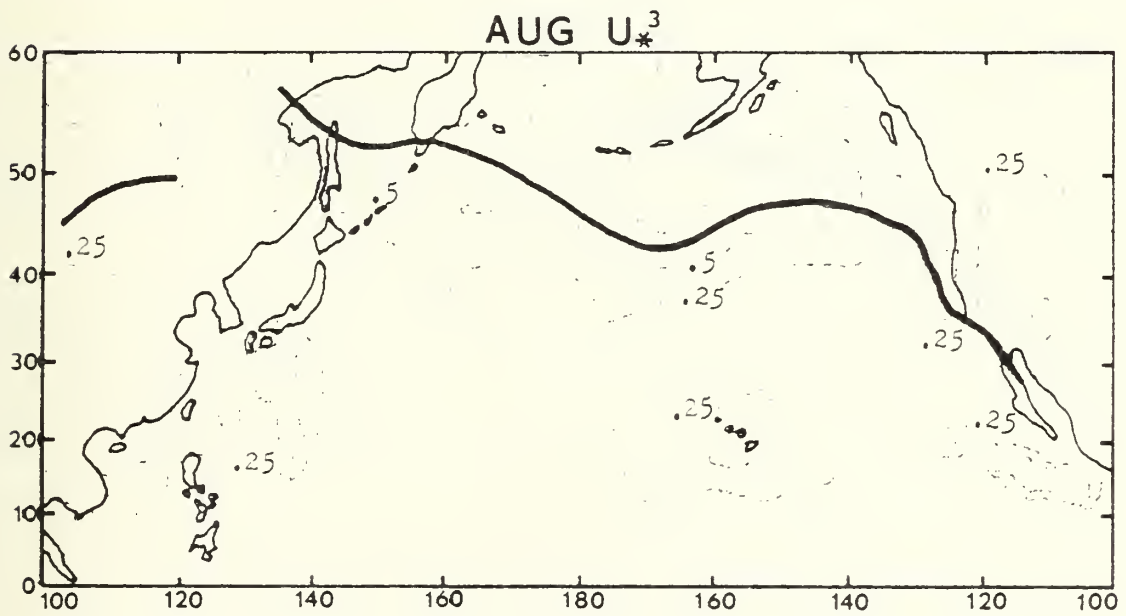


Figure 17. Same as Fig. 3 except for August 1975.





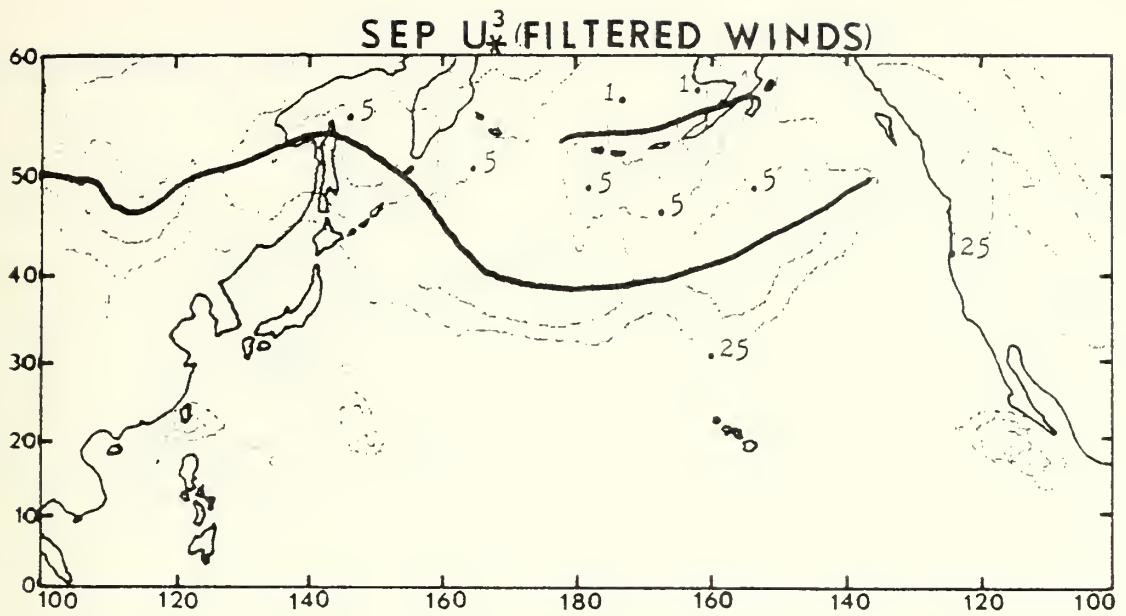


Figure 18. Same as Fig. 2 except for September 1975.

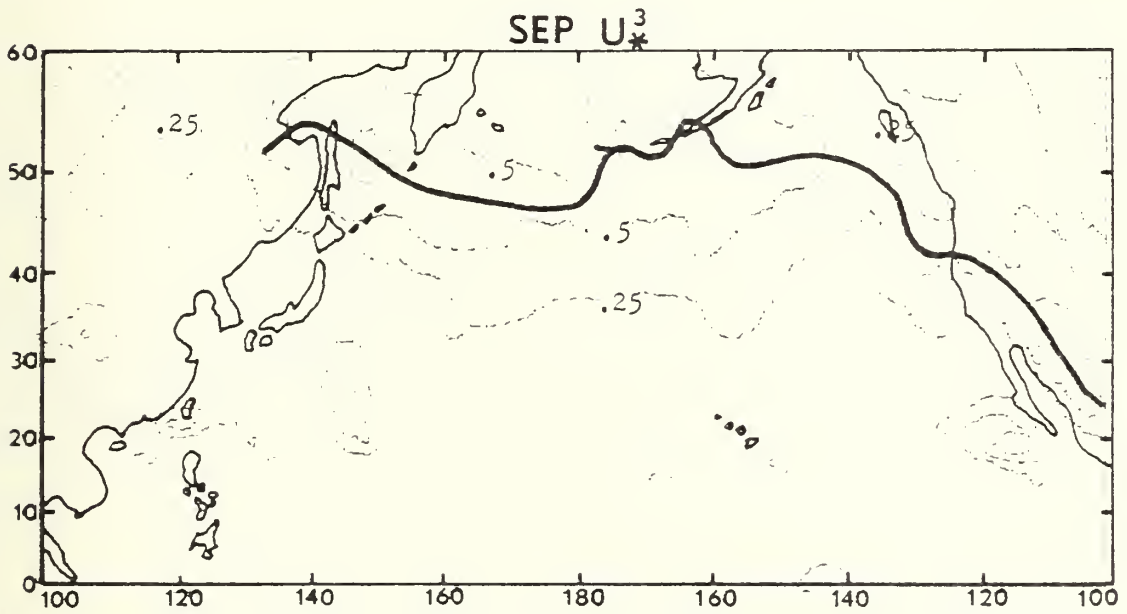


Figure 19. Same as Fig. 3 except for September 1975.



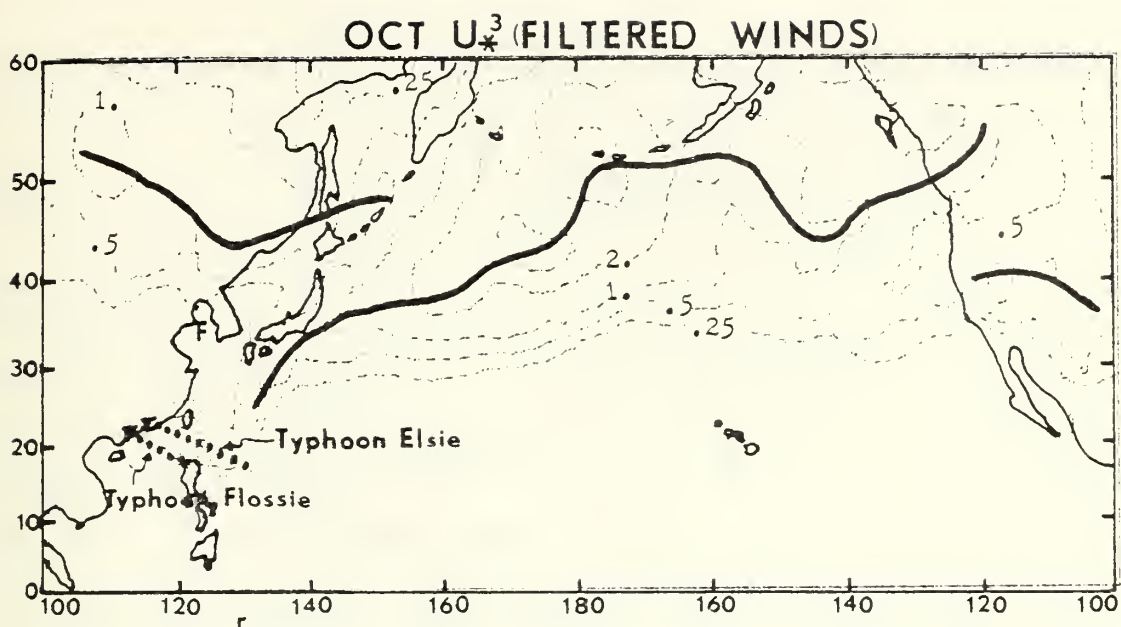


Figure 20. Same as Fig. 2 except for October 1975, and the paths of Typhoons Elsie and Flossie are shown.

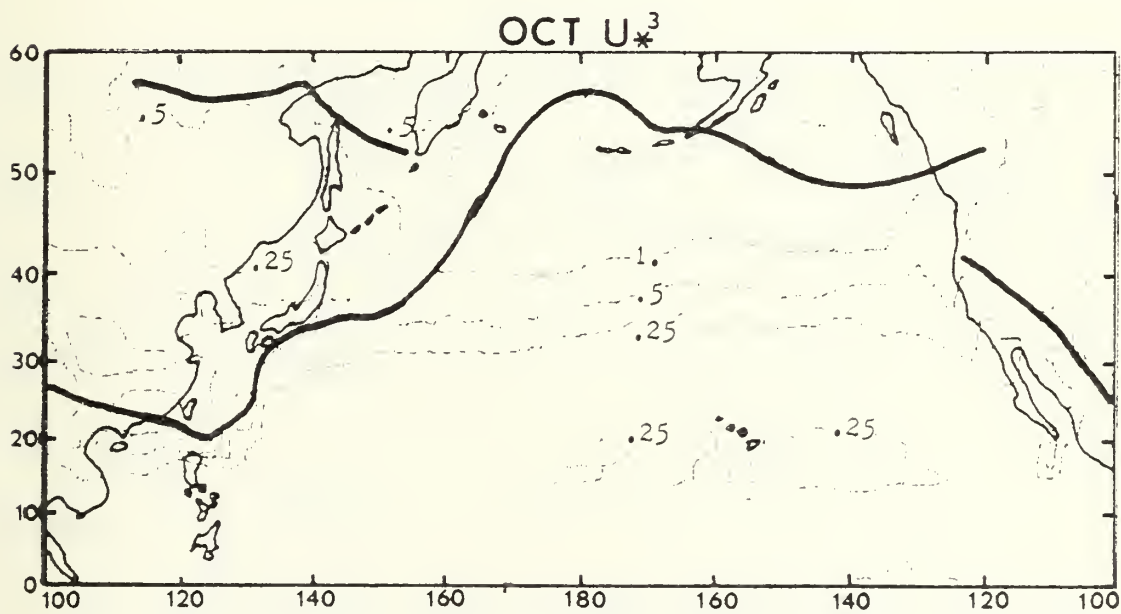


Figure 21. Same as Fig. 3 except for October 1975.



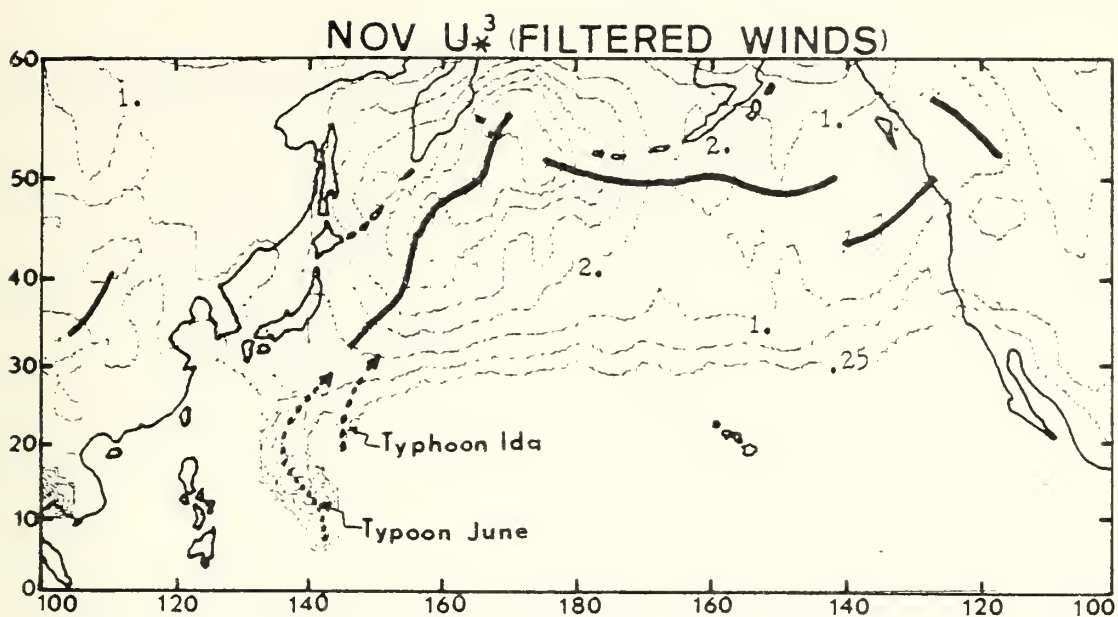


Figure 22. Same as Fig. 2 except for November 1975, and the paths of Typhoons June and Ida are shown.

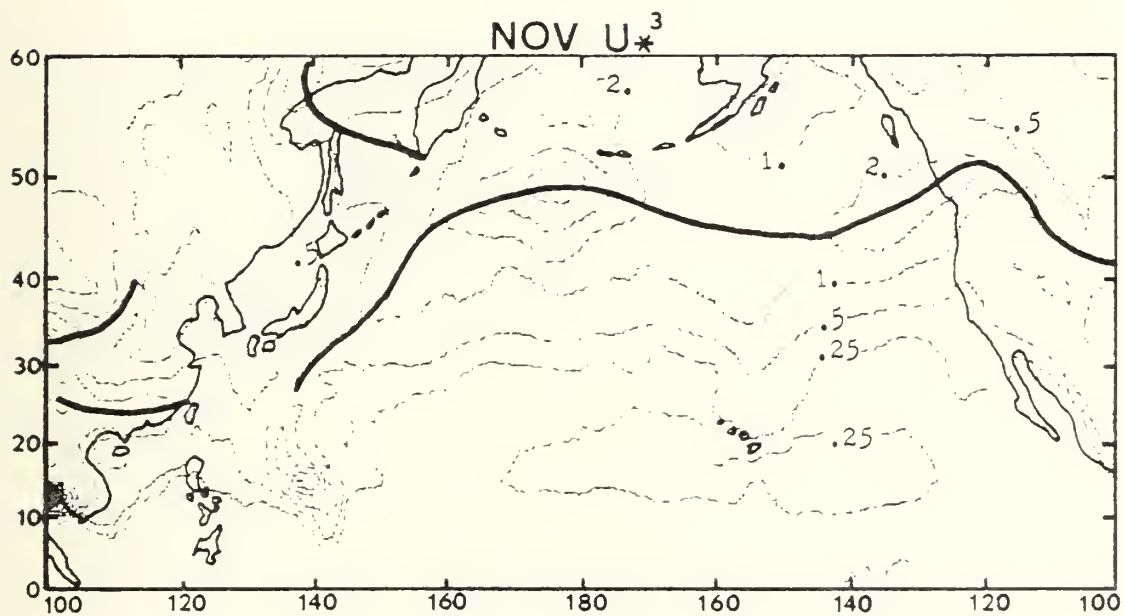


Figure 23. Same as Fig. 3 except for November 1975.



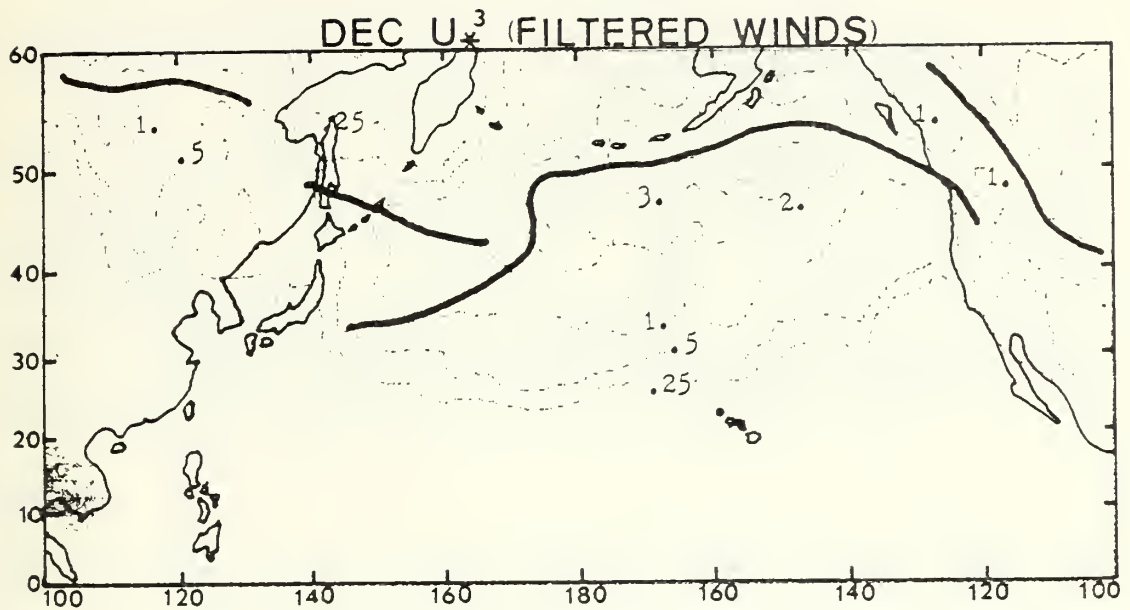


Figure 24. Same as Fig. 2 except for December 1975.

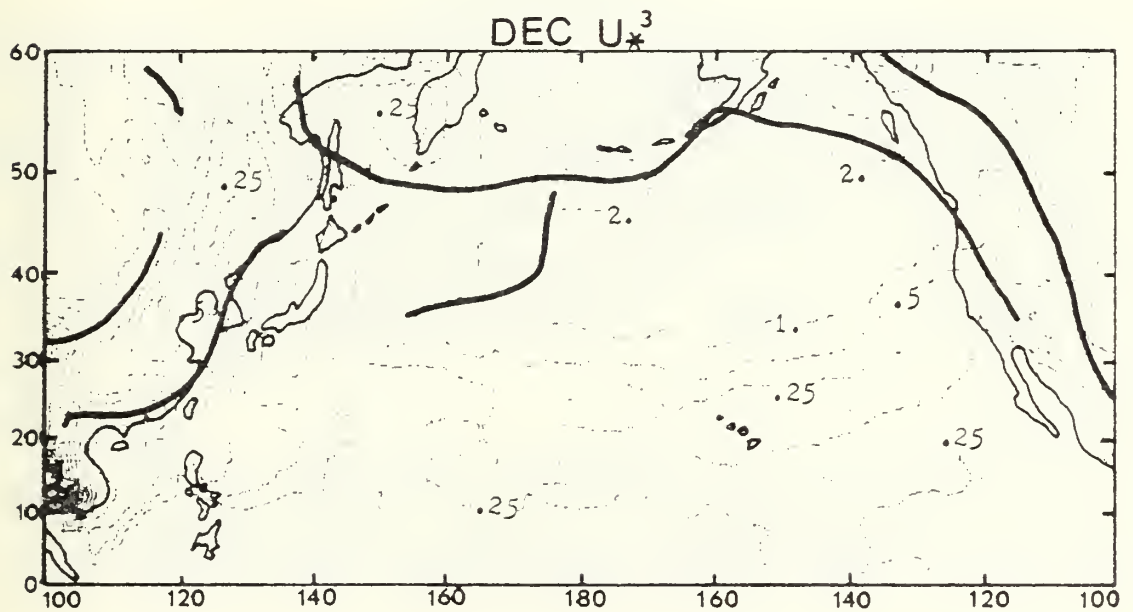


Figure 25. Same as Fig. 3 except for December 1975.





# JAN $\text{CURL}_z \tau$ (FILTERED WINDS)

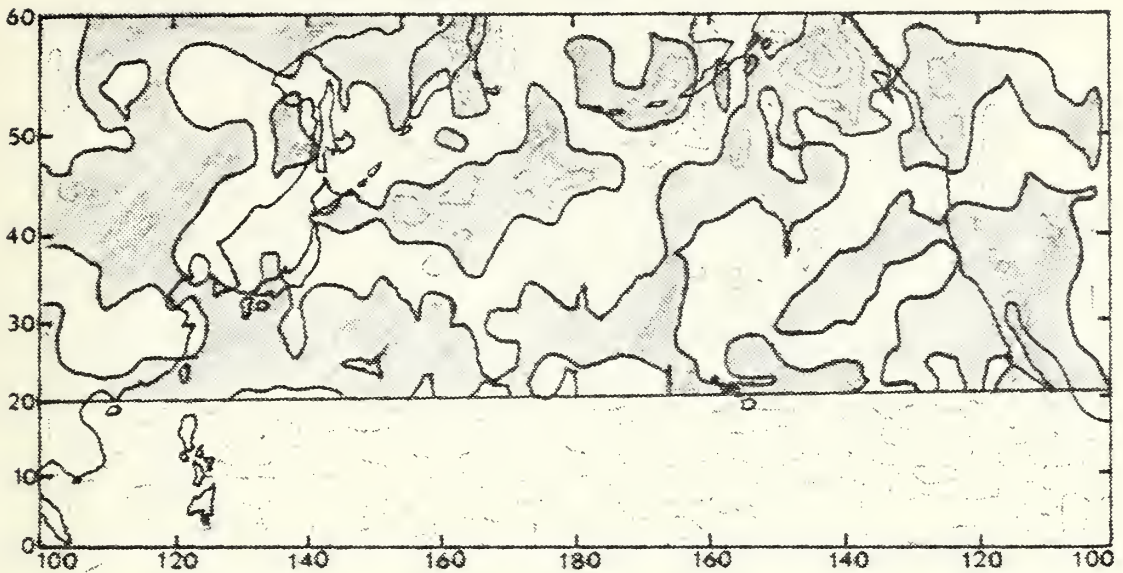


Figure 26. The vertical component of the January monthly mean wind stress curl ( $\text{curl}_z \tau$ ) from band pass filtered u and v wind components. Contour values are  $-4., -3., -2., -1., \pm 0., +1., +2., +3., +4. \times 10^{-9}$  dynes/cm<sup>3</sup>. The heavy lines are lines of zero curl, and gray shading denotes positive curl.

# JAN $\text{CURL}_z \tau$

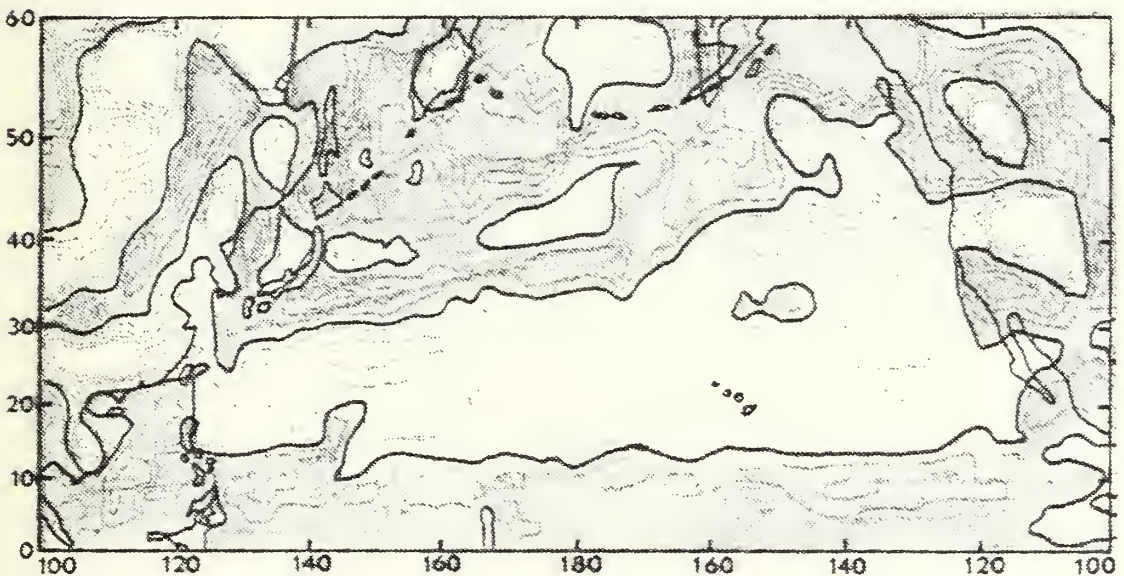


Figure 27. The vertical component of the January monthly mean wind stress curl ( $\text{curl}_z \tau$ ) from unfiltered u and v wind components. Contour values are as in Fig. 26 except values are times  $10^{-8}$  dynes/cm<sup>3</sup>. The heavy lines are lines of zero curl.



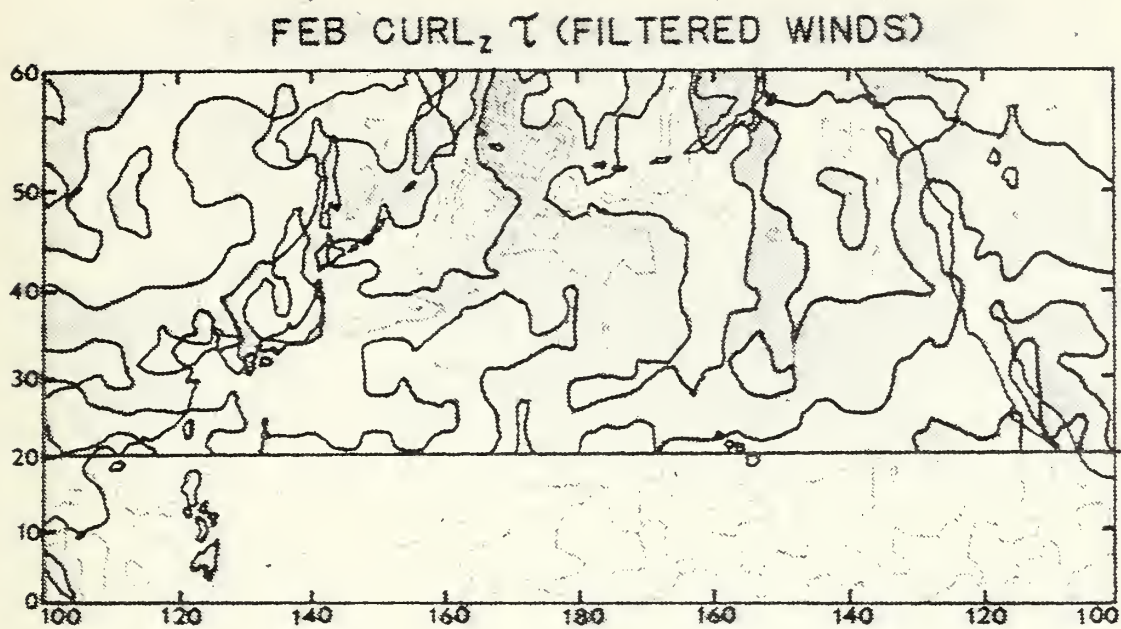


Figure 28. Same as Fig. 26 except for February 1975.

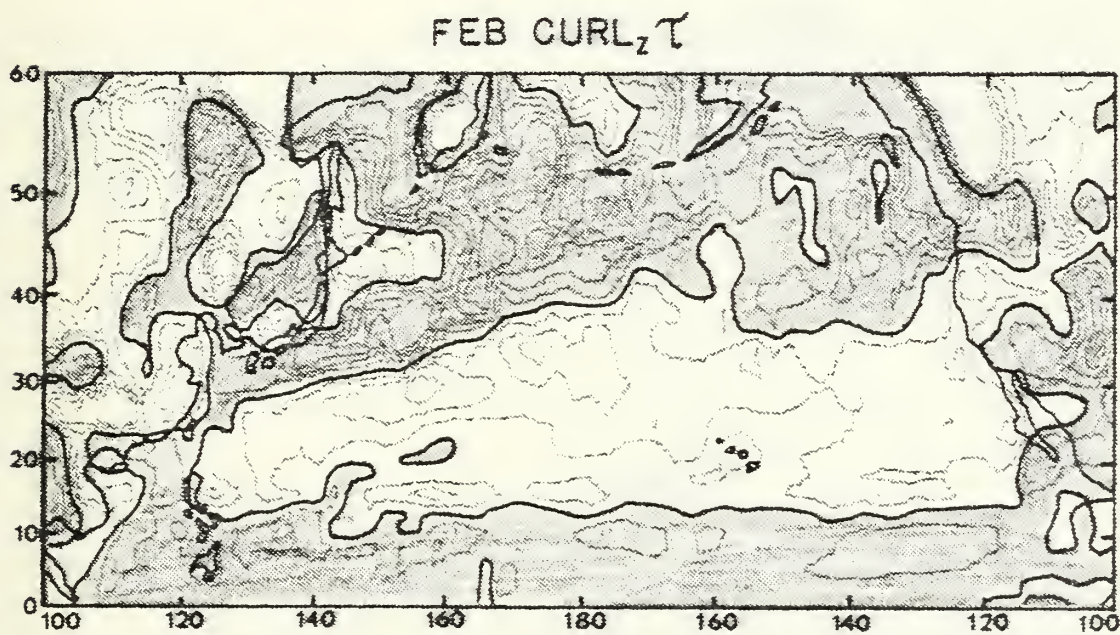


Figure 29. Same as Fig. 27 except for February 1975.





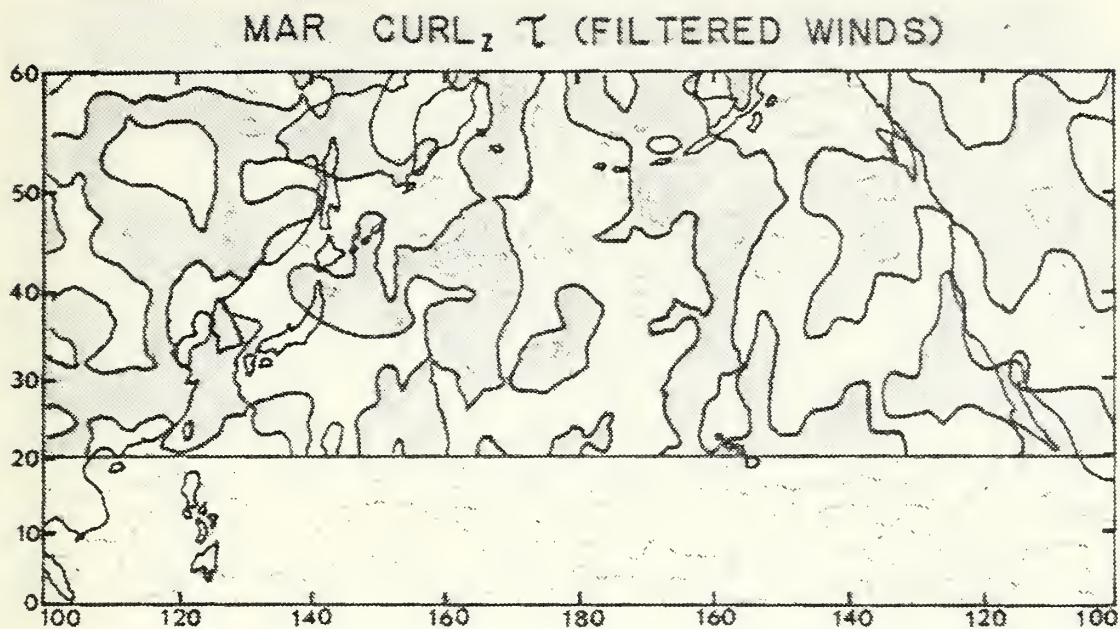


Figure 30. Same as Fig. 26 except for March 1975.

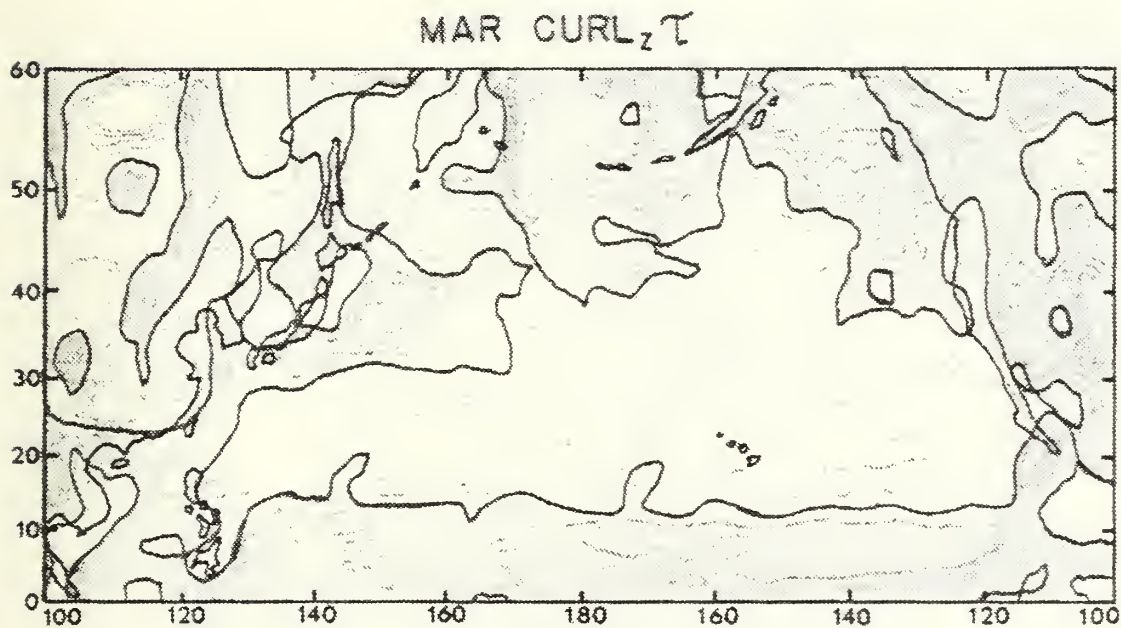


Figure 31. Same as Fig. 27 except for March 1975.



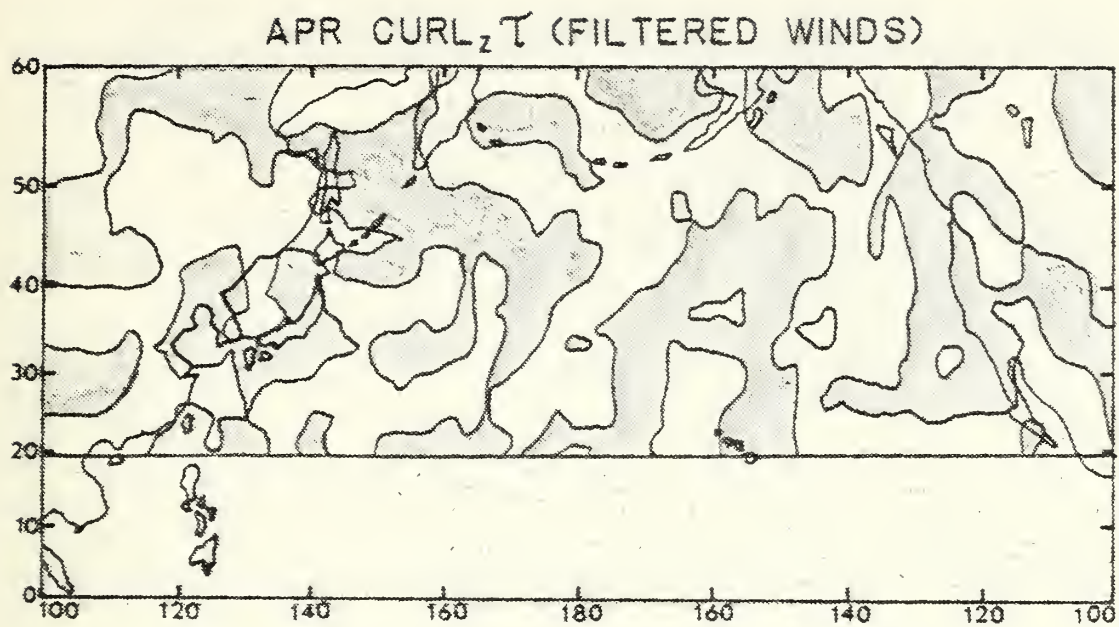


Figure 32. Same as Fig. 26 except for April 1975.

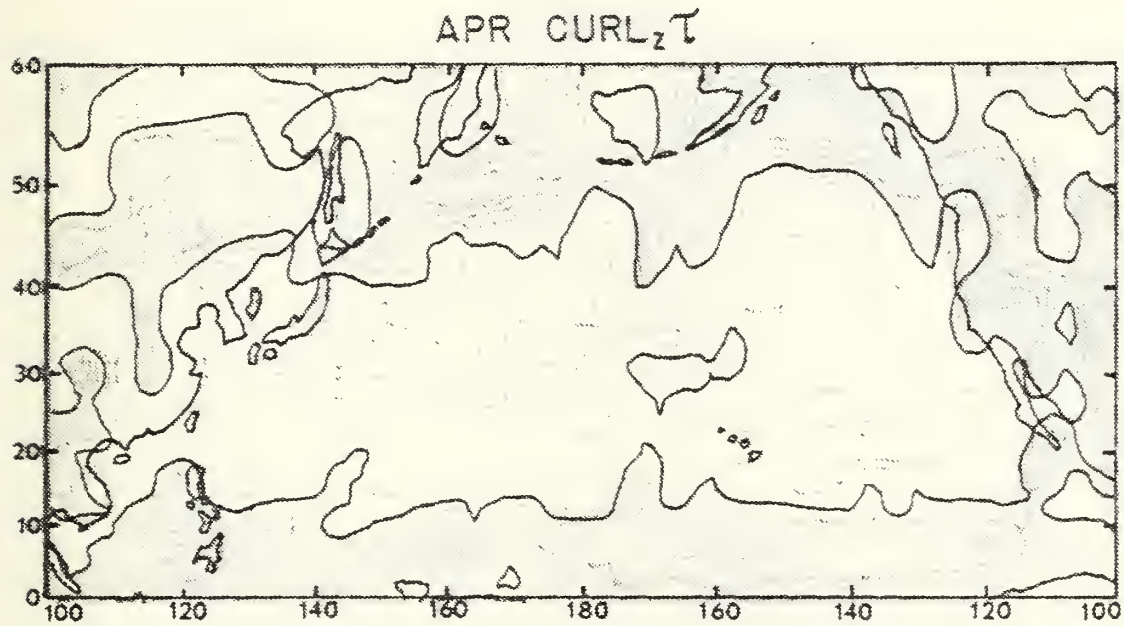


Figure 33. Same as Fig. 27 except for April 1975.





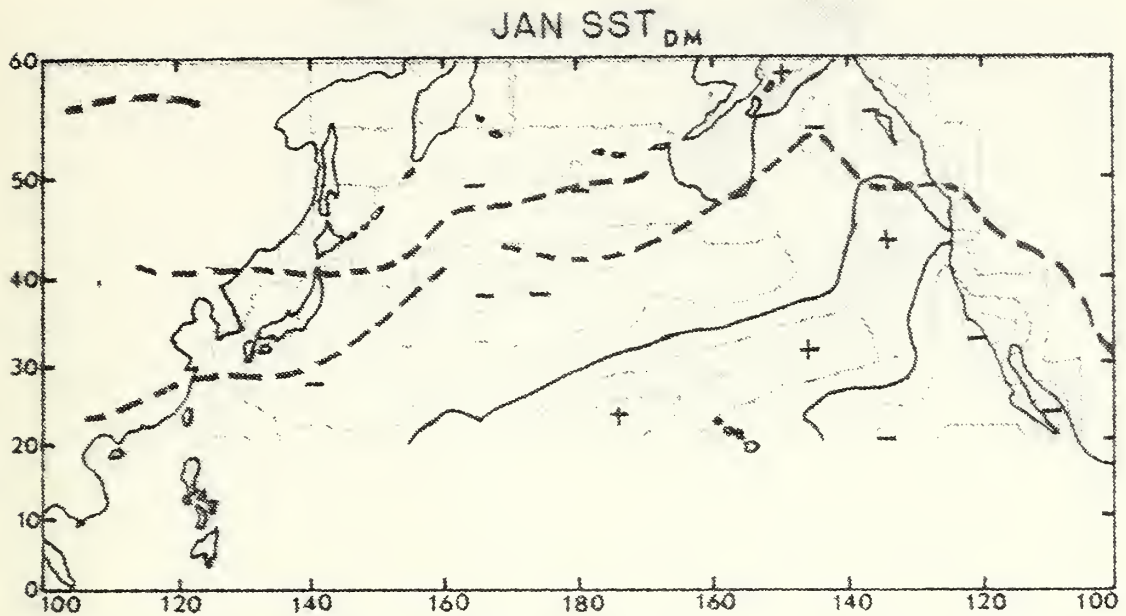


Figure 34. January monthly mean sea surface temperature anomalies ( $SST_{DM}$ ). Contour intervals are  $.5^{\circ}C$ . Heavy lines are zero anomaly lines, warm anomaly areas are denoted by +, and cold anomaly areas are denoted by -. Dashed lines indicate monthly mean maximum areas of  $u_*^3$  from filtered wind as in Fig. 2.

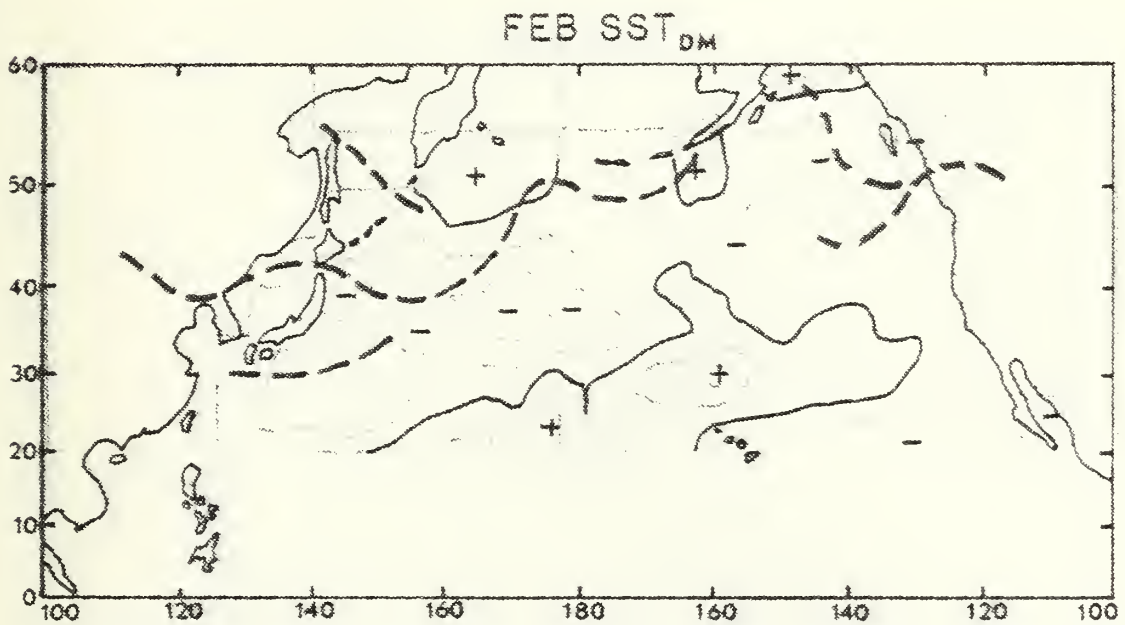


Figure 35. Same as Fig. 34 except for February 1975.



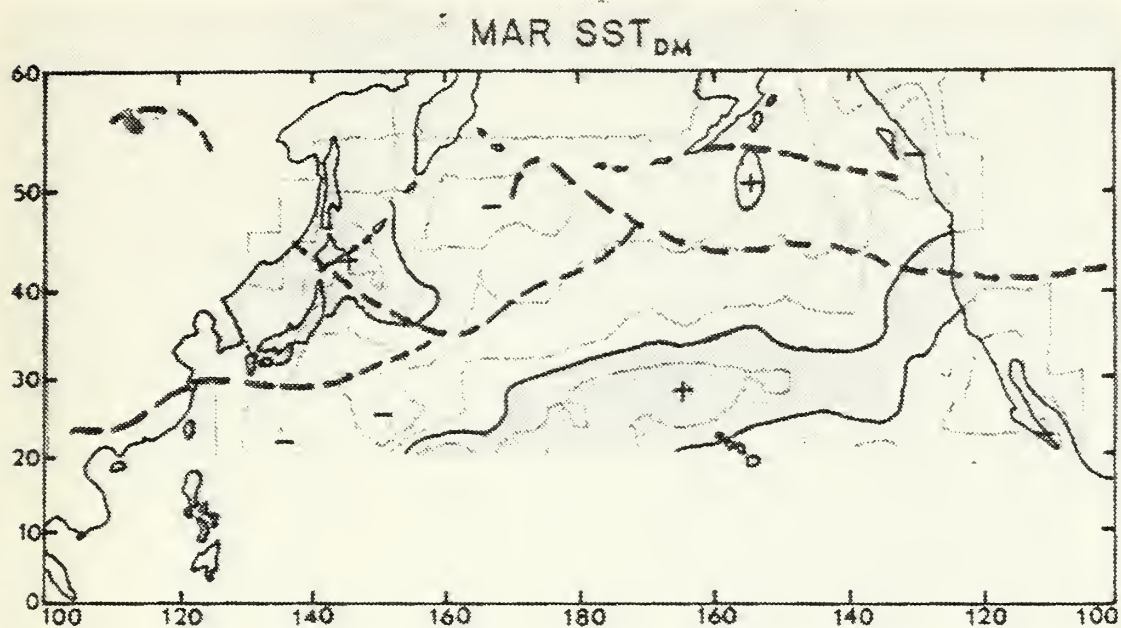


Figure 36. Same as Fig. 34 except for March 1975.

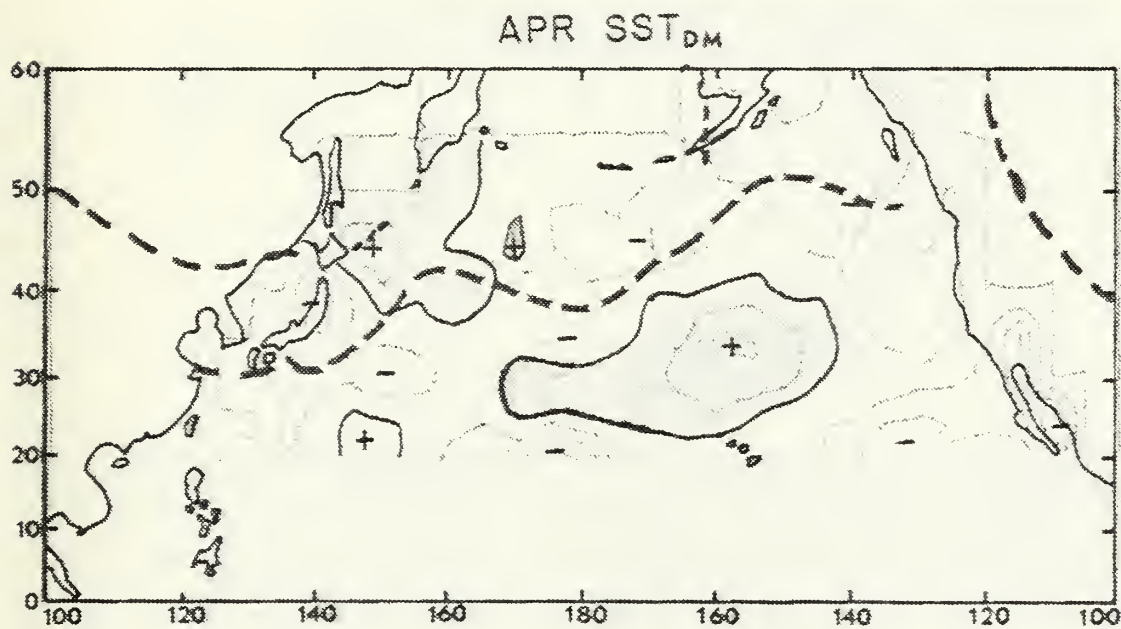


Figure 37. Same as Fig. 34 except for April 1975.



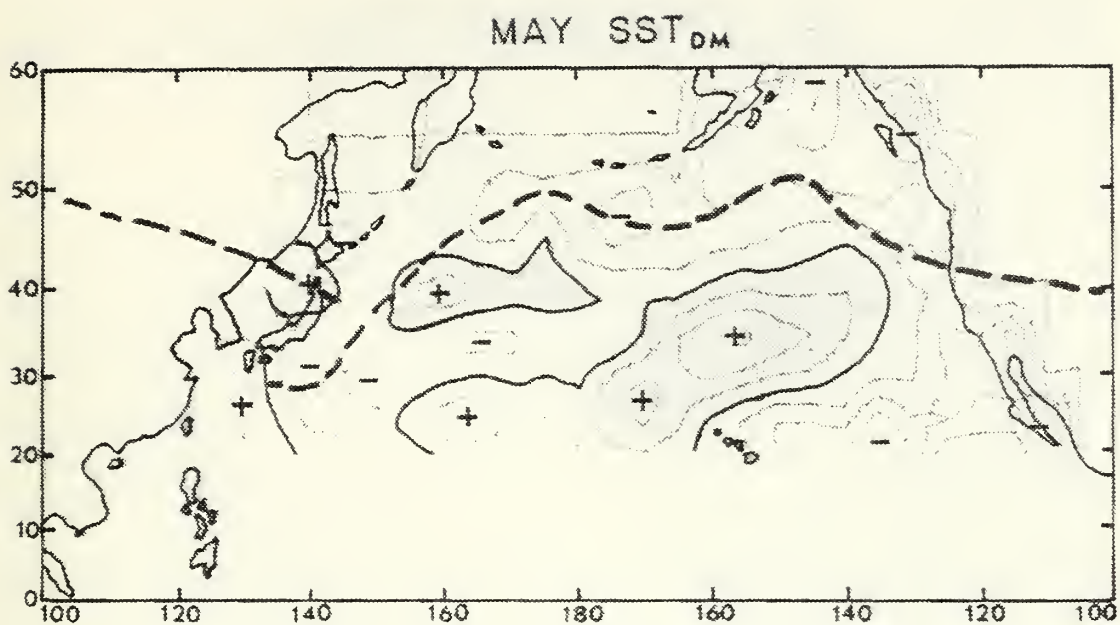


Figure 38. Same as Fig. 34 except for May 1975.

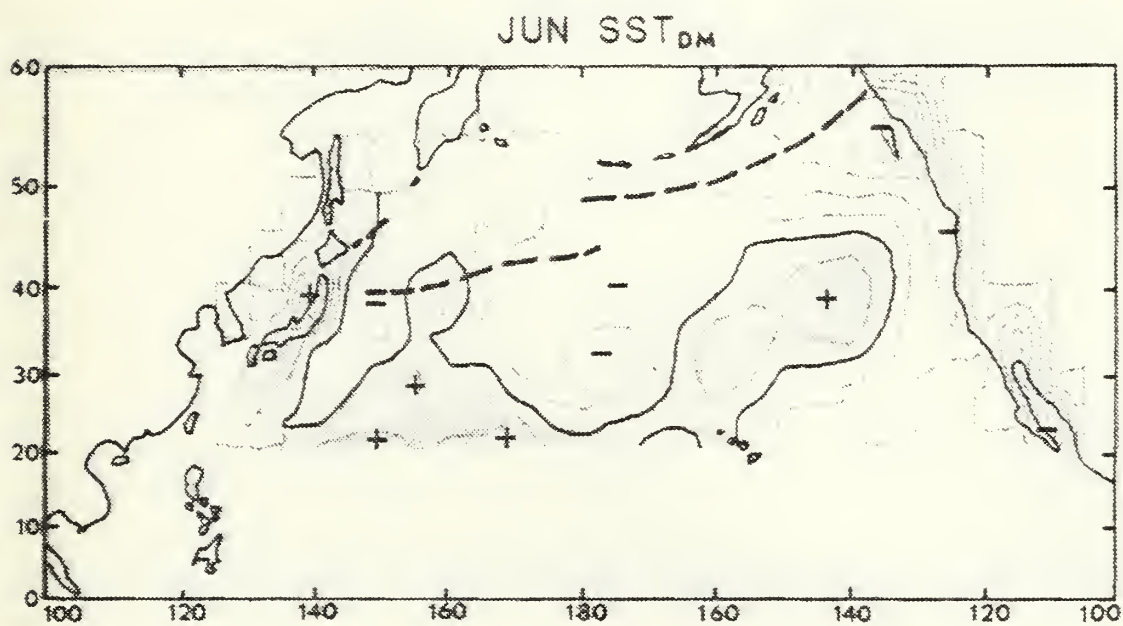


Figure 39. Same as Fig. 34 except for June 1975.





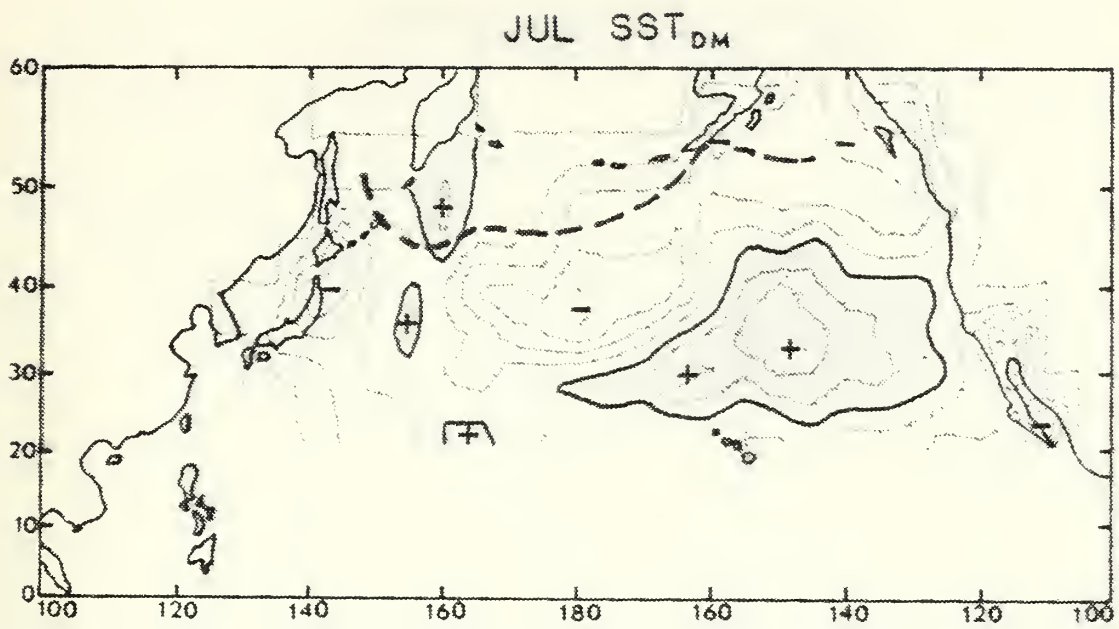


Figure 40. Same as Fig. 34 except for July 1975.

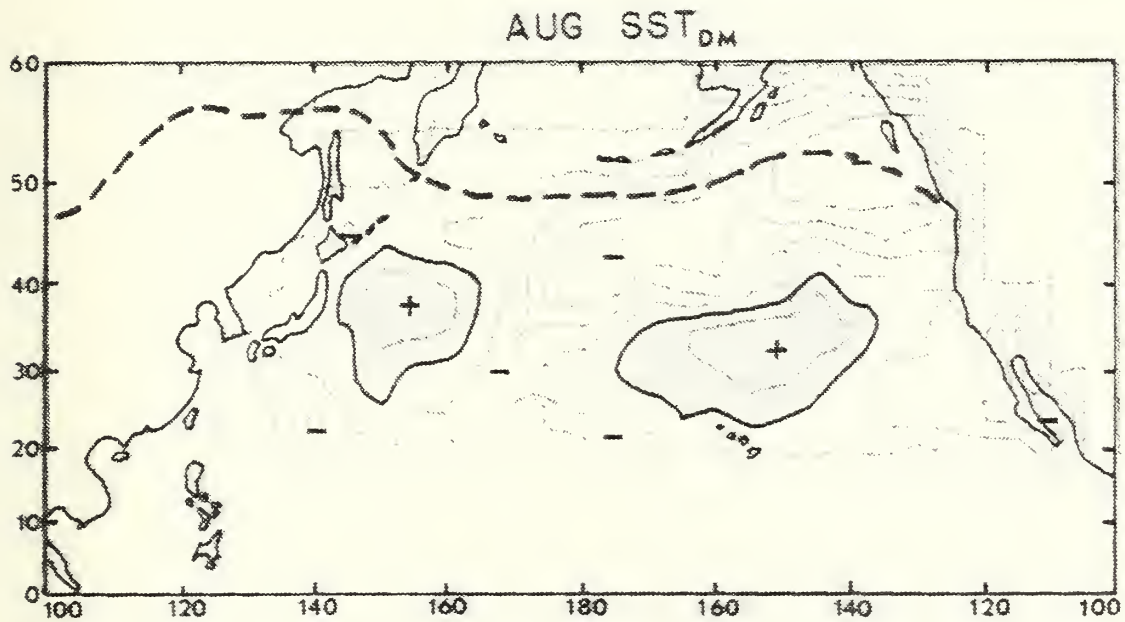


Figure 41. Same as Fig. 34 except for August 1975.





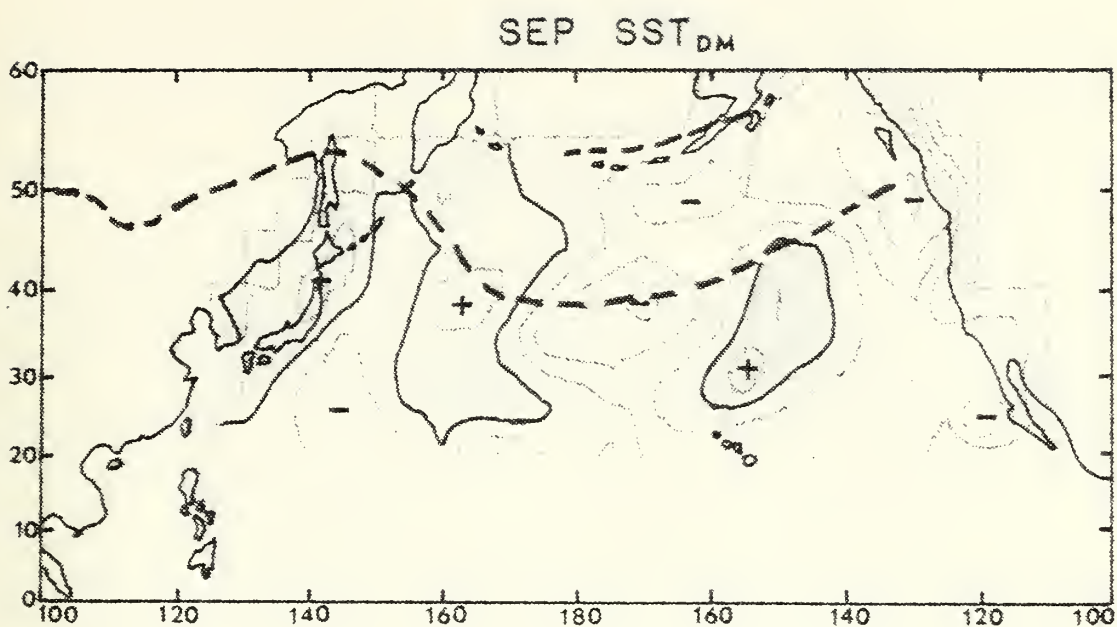


Figure 42. Same as Fig. 34 except for September 1975.

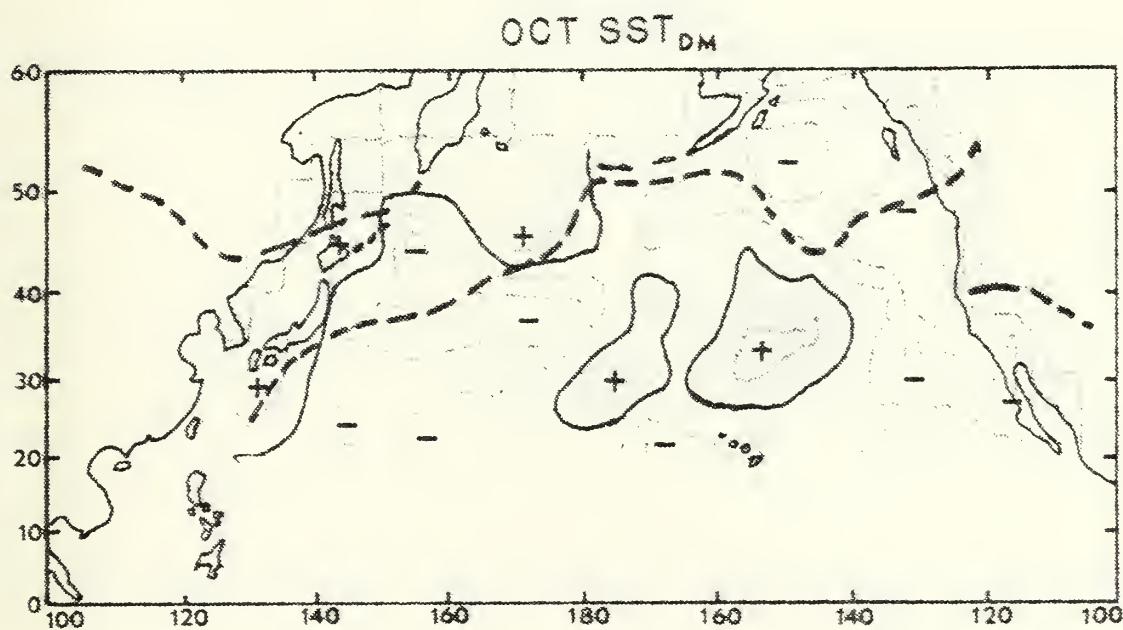


Figure 43. Same as Fig. 34 except for October 1975.



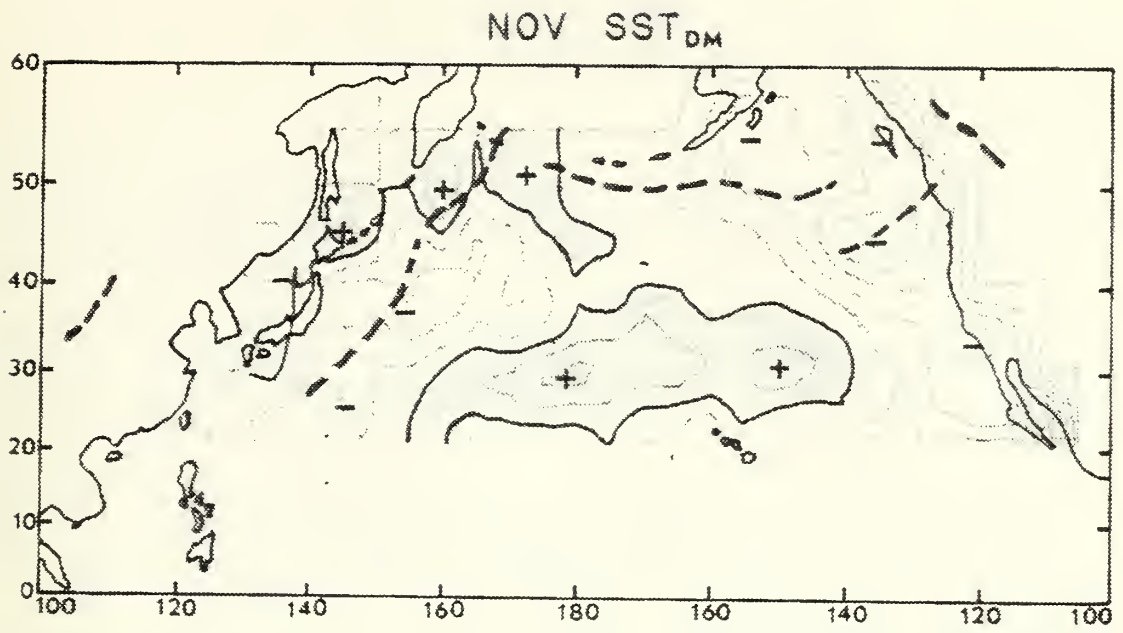


Figure 44. Same as Fig. 34 except for November 1975.

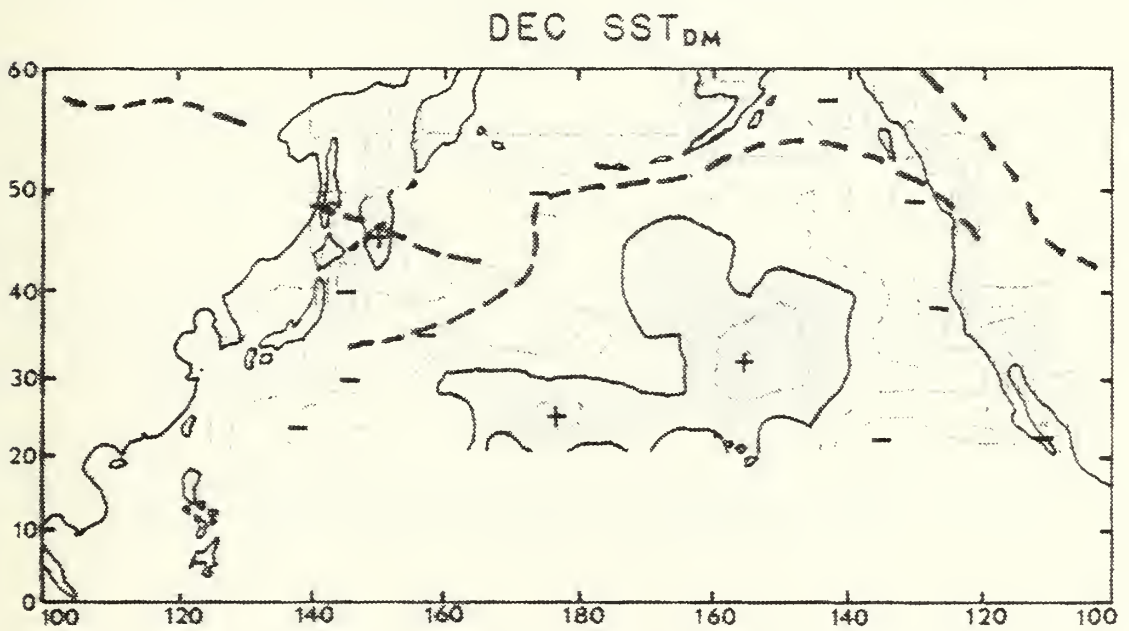


Figure 45. Same as Fig. 34 except for December 1975.



## LIST OF REFERENCES

- Blackmon, M.  
1976. A climatological spectral study of the 500 mb geopotential height of the northern hemisphere, J. Atmos. Sci., 33, 1607-1623.
- Camp, N. T., and R. L. Elsberry.  
1977. Ocean thermal response to strong atmospheric forcing. II. The role of one-dimensional processes. Accepted by J. Phys. Oceanogr.
- Davis, R.  
1976. Predictability of sea surface temperature and sea level pressure anomalies over the North Pacific Ocean, J. Phys. Oceanogr., 6, 249-266.
- U. S. Naval Weather Service Numerical Environmental Products Manual, 1975.  
1975. Fleet Numerical Weather Central, Monterey, CA 93940.
- Joint Typhoon Warning Center, 1975.  
1975. Annual Typhoon Report. U. S. Fleet Weather Central, Joint Typhoon Warning Center, COMNAVMARIANAS, Box 12, FPO San Francisco, 96630.
- Pazan, S.  
1977. Anomaly Dynamics Study, Report Number 1. Scripps Institution of Oceanography, Univ. of California, S.I.O. reference number 77-19.
- Namias, J.  
1972. Large-scale and long-term fluctuations in some atmospheric and oceanic variables. Nobel Symposium 20, D. D. Dyrssen and D. D. Jagner, Eds. Almqvist and Wiksell, Stockholm, 27-48.
- Simpson, J.  
1969. On some aspects of sea-air interaction in middle latitudes. Deep Sea Research Supplement, 16, 233-261.



# INITIAL DISTRIBUTION LIST

	No. Copies
1. Defense Documentation Center Cameron Station Alexandria, Virginia 22314	2
2. Library, Code 0142 Naval Postgraduate School Monterey, California 93940	2
3. Dr. G. J. Haltiner, Code 63Ha Department of Meteorology Naval Postgraduate School Monterey, California 93940	1
4. Dr. R. L. Haney, Code 63Hy Department of Meteorology Naval Postgraduate School Monterey, California 93940	2
5. Director, Naval Oceanography and Meteorology Building 200 Washington Navy Yard Washington, D. C. 20374	1
6. Meteorology Department Code 63 Library Naval Postgraduate School Monterey, California 93940	1
7. Dr. M. Miyake Institute of Oceanography University of British Columbia Vancouver, Canada V6% 1W5	1
8. Prof. J. M. Wallace Department of Atmospheric Sciences University of Washington Seattle, Washington 98195	1
9. Dr. J. Namias Scripps Institution of Oceanography University of California, San Diego La Jolla, California 92093	1
10. Maj. J. Pavone AWS/DOR Scott AFB, Illinois 62225	1





- |     |                                  |   |
|-----|----------------------------------|---|
| 11. | Air Weather Service              | 1 |
|     | AWS/TF                           |   |
|     | Scott AFB, Illinois 62225        |   |
| 12. | Capt. Harry Hughes               | 2 |
|     | AFIT/CIPF                        |   |
|     | Wright-Patterson AFB, Ohio 45433 |   |
| 13. | Capt. Gary C. Heise              | 2 |
|     | 12905 South 31st Street          |   |
|     | Omaha, Nebraska 68123            |   |



172731

Thesis  
H4238  
c.1

Heise

A statistical study  
of synoptic storm  
activity over the  
north Pacific in 1975.

Thesis  
H4238  
c.1

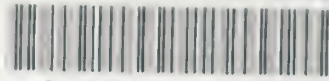
Heise

172731

A statistical study  
of synoptic storm  
activity over the  
north Pacific in 1975.

thesH4238

A statistical study of synoptic storm ac



3 2768 001 91804 8

DUDLEY KNOX LIBRARY